

Effective and flexible depth-based inference for functional parameters

Hyemin Yeon*

Abstract

For hypothesis testing of functional parameters, given a functional statistic T_n and a functional depth D with respect to the distribution P_n of T_n , we propose the depth value $DT_n \equiv D(T_n; P_n)$ as a test statistic, which we refer to as a *depth statistic*. In practice, its sampling distribution is approximated by a resampling method such as bootstrap. While achieving accurate sizes, a test based on the proposed depth statistic produces stronger power, as it remains sensitive even to subtle variations arising from complex functional patterns in the alternatives. Moreover, it is broadly applicable to a broad range of inference problems for functional parameters, including two-sample tests, analysis of variance, regression, etc. We provide its theoretical guarantee under mild assumptions along with examples of bootstrap methods and functional depths that satisfy these conditions. Its effectiveness is thoroughly investigated through numerical studies under two popular frameworks: (i) two-sample functional mean tests and (ii) mean response inference for function-on-function regression. The proposed depth statistic is illustrated with two data examples: Canadian weather and German electricity prices datasets.

Keywords and phrases: Data depth, Functional data analysis, Infinite-dimensional parameters; Shape alternatives.

*Department of Mathematical Sciences, Kent State University, Kent, OH, 44242, USA,
Email: hyeon1@kent.edu.

1 Introduction

1.1 Background

In functional data analysis, statistical inference for functional parameters is challenging due to infinite dimensionality of the underlying function space. Nevertheless, numerous meaningful advances have been made. These include (a) confidence bands for functional parameters by [Choi and Reimherr \(2018\)](#), [Degras \(2011\)](#), [Liebl and Reimherr \(2023\)](#), (b) two-sample tests for equality of (i) means by [Benko et al. \(2009\)](#), [Bunea et al. \(2011\)](#), [Dette et al. \(2020\)](#), [Horváth et al. \(2013\)](#), [Pini et al. \(2018\)](#), (ii) covariance operators by [Fremdt et al. \(2013\)](#), [Kraus and Panaretos \(2012\)](#), [Panaretos et al. \(2010\)](#), and (iii) eigenvalues or eigenfunctions by [Aue et al. \(2023\)](#), [Benko et al. \(2009\)](#), [Zhang and Shao \(2015\)](#), (c) functional ANOVA for (i) several means by [Cuesta-Albertos and Febrero-Bande \(2010\)](#), [Cuevas et al. \(2004\)](#), [Górecki and Smaga \(2015\)](#), [Horváth and Rice \(2015\)](#), [Lin et al. \(2023\)](#), [Paparoditis and Sapatinas \(2016\)](#), [Zhang and Liang \(2014\)](#), [Zhang et al. \(2019\)](#) and (ii) multiple covariance operators by [Boente et al. \(2018\)](#), [Guo et al. \(2019\)](#), [Masarotto et al. \(2024\)](#), [Paparoditis and Sapatinas \(2016\)](#), (d) tests of equality between distributions by [Chen et al. \(2025\)](#), [Hall and Van Keilegom \(2007\)](#), [Hlávka et al. \(2022\)](#), [Wynne and Duncan \(2022\)](#), (e) significance tests for contrast functions in (f) function-on-scalar regression models by [Faraway \(1997\)](#), [Shen and Faraway \(2004\)](#), [Zhang \(2011\)](#), [Zhang and Chen \(2007\)](#) and (g) functional concurrent regression models by [Ghosal and Maity \(2022\)](#), [Wang et al. \(2018\)](#), (h) inference for mean response or slope operator in function-on-function regression models by [Crambes and Mas \(2013\)](#), [Dette and Tang \(2024\)](#), [Kokoszka et al. \(2008\)](#), [Yeon \(2026+\)](#). Classical summary statistics in this literature often take the form of quadratic structures incorporating eigendecay (e.g., truncated Hotelling's T^2), integration (e.g., squared L^2 norm), supremum (e.g., supremum of pointwise F statistics), or their variants, where their performance can be enhanced by resampling methods such as bootstrap.

Complementary to inference for functional parameters, considerable attention has also been devoted to the study of functional depths. Originally introduced in multivariate statistics ([Chaudhuri, 1996](#), [Liu, 1990](#), [Mosler, 2002](#), [Tukey, 1975](#), [Zuo, 2003](#)), the notion of data depth has been extended to functional data, leading to proposals such as integrated ([Fraiman and Muniz, 2001](#)), kernel (or h -mode) ([Cuevas et al., 2006](#)), (modified) band ([López-Pintado and Romo, 2009](#)), half-region ([López-Pintado and Romo, 2011](#)), infimal ([Mosler, 2013](#)), spatial ([Chakraborty and Chaudhuri, 2014](#)), extremal ([Narisetty and Nair, 2016](#)), regularized Mahalanobis ([Berrendero et al., 2020](#)), L^2 ([Ramsay and Chenouri, 2024](#)), spherical ([Mendroš and Nagy, 2025](#)), and regularized halfspace ([Yeon et al., 2025](#)) depths; see [Section 4](#) for a brief overview of some selective functional depths. These constructions provide rankings of complex functional observations that capture the geometry of the underlying distribution, beyond simple balls or ellipsoids determined solely by norms or quadratic forms. Func-

tional depths have enabled a wide range of statistical applications such as rank-based tests (Gnettner et al., 2024), classification (Hubert et al., 2017), and outlier detection (Nagy et al., 2017). Since there have been thousands of contributions in the vast literature on both (i) inference for functional parameters and (ii) functional depths, we do not attempt an exhaustive review here.

1.2 Depth statistic for functional parameters

In this work, we propose using the depth evaluated at a statistic, as a test statistic for general statistical inference problems for functional parameters. This approach will be able to bridge the aforementioned two active communities: inference for functional parameters and depth for functional data. Concretely, given (i) a test statistic T_n to test a hypothesis $H_0 : \theta = \theta_0$ about a functional parameter θ and (ii) a functional depth D at hand, we define the depth statistic as $DT_n \equiv D(T_n; P_n)$, the depth value evaluated at T_n with respect to its sampling distribution P_n , where small values of DT_n support evidence against H_0 . Although the sampling distribution of the depth statistic DT_n cannot be explicitly provided, we employ resampling methods to approximate them, such as well-established bootstrap methods for functional data (e.g., Benko et al., 2009, Paparoditis and Sapatinas, 2016, Yeon, 2026+). The proposed depth statistic then leads to valid inference tools for functional parameters, as long as (i) the resampled distribution \hat{P}_n consistently estimate the original sampling distribution P_n with limiting distribution P , (ii) the functional depth possesses uniform continuity in either element or probability distribution, and (iii) the depth value at the limiting random element with respect to P is continuous.

The depth statistic exploits the entire ordering structure of the sampling distribution for hypothesis testing. It offers not only accurate sizes but also greater power than classical summary statistics, which often fail to detect complex alternatives whose signals hindered by complexity in functional data. To illustrate, we consider a realization of 50 curves under the two-sample functional mean framework (Example 1(a)), with 25 curves per group (cf. Section 5.1). Figure 1 displays the two-sample test statistic $T_{\text{two},n} = \bar{X}_1 - \bar{X}_2$ in green, the true mean difference $\theta = \mu_1 - \mu_2$ in red, and 1,000 bootstrap statistics $T_{\text{two},n}^* = \bar{X}_1^* - \bar{X}_2^*$ (cf. Section 3.1) in gray. Although the problem is challenging because the group means differ only in shape, the depth statistics effectively capture subtle functional alternatives, with the regularized halfspace depth and kernel depth (cf. Section 4) yielding p-values below the significance level 0.05 (0.000 for the former with quantile level 0.1 and 0.009 for the latter with quantile level 0.01). In contrast, classical statistics often struggle to detect complex signals in functional alternatives, as illustrated by the commonly used L^2 and supremum norm-based tests. In Figure 1, the 95% confidence band constructed from the supremum norm (shown in blue), with critical values calibrated via bootstrap statistics, still contains zero even though the true mean difference deviates from zero in shape, yielding a p-value

of 0.098. This indicates that the supremum statistic fails to capture the functional characteristic in shape. Similarly, the L^2 statistic produces a p-value above the 0.05 significance level (0.081). Further details on the superior performance of the proposed depth statistics are provided in [Section 5](#).

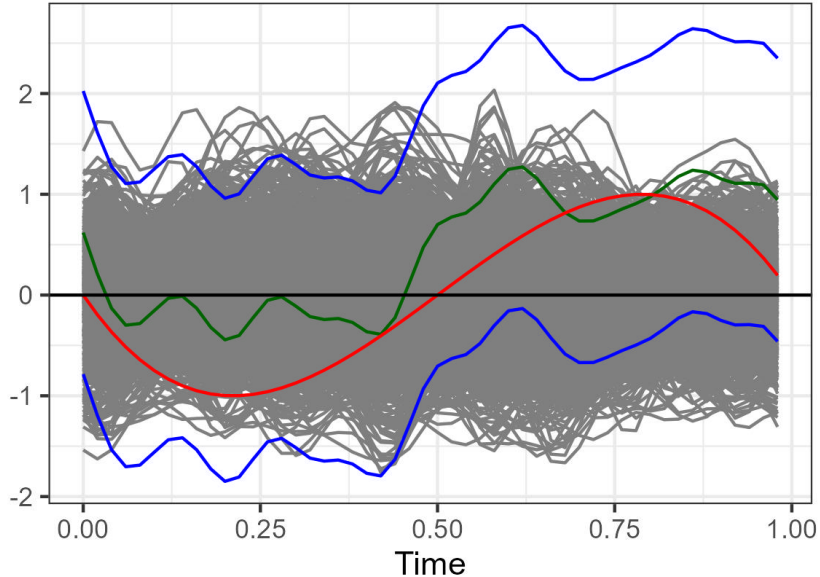


Figure 1: The test statistic $T_{\text{two},n} = \bar{X}_1 - \bar{X}_2$ (green), bootstrap statistics $T_{\text{two},n}^* = \bar{X}_1^* - \bar{X}_2^*$ (grey), and the true mean difference $\theta = \mu_1 - \mu_2$ (red, cubic alternative). The black horizontal line at zero stands for the true mean difference in the null hypothesis $H_0 : \mu_1 = \mu_2$. The $n_k = 25$ functional observations in each group k are generated as described in [Section 5.1](#) under equal covariance scenario when the functional principal components are of NN-type. The details about the two-sample bootstrap procedure can be found in [Section 3.1](#).

Beyond its effectiveness, the proposed depth statistic is broadly applicable to general inference problems for functional parameters. It provides valid tools whenever the functional depth is well-estimated and the resampling distribution consistently approximates the sampling distribution. In [Section 3](#), we present several functional inference frameworks, including those discussed above, and highlight two fundamental applications: (i) two-sample functional mean testing and (ii) mean response inference in function-on-function regression. Their theoretical foundations and numerical performance are detailed in [Sections 3](#) and [5](#), respectively.

In developing our functional depth statistic DT_n , we noted related ideas for multivariate data by [Liu and Singh \(1997, depth p-value\)](#) and [Yeh and Singh \(1997, depth confidence region\)](#), yet there are several unique distinctions of our proposal. First, the depth statistic is defined at the population level, whereas the concepts in [Liu and Singh \(1997\)](#), [Yeh and Singh \(1997\)](#) exist only at the bootstrap level. Second, establishing validity for functional parameters could be nontrivial due to their infinite dimensionality. For instance, a bootstrap may fail when infinite dimension is involved ([Yeon et al., 2024](#)) and a depth consistency rarely

holds over an entire infinite-dimensional space (Wynne and Nagy, 2025). Nevertheless, we provide important examples satisfying all sufficient conditions for our main result in [Theorem 1](#), which offers a stronger form than [Liu and Singh \(1997, Theorem 1\)](#). Third, the practical advantages of the functional depth statistic are more pronounced, since functional alternatives are far less easily detectable than finite-dimensional ones (cf. [Figure 1](#)). Fourth, to the best of our knowledge, depth-based inference has not previously been studied for functional parameters. Finally, no comprehensive power analysis has been conducted in numerical studies, further underscoring the novelty of our contribution.

1.3 Organization of the paper

The structure of the paper is organized as follows. After summarizing preliminary notation, in [Section 2](#), the formal definition of the proposed functional depth statistic is presented along with its theoretical validity. [Sections 3 and 4](#) then provide various examples of inference problems and depth for functional data, where our framework is applicable. Importantly, we found some cases that satisfies our technical conditions. Namely, we develop detailed procedures for functional depth-based inference in the contexts of two-sample testing and function-on-function regression in [Section 3](#); and we establish continuity properties of a functional depth in [Section 4](#). [Section 5](#) reports numerical power analyses that demonstrate the superiority of the proposed depth statistic, while [Section 6](#) provides empirical illustrations using real data. All proofs are deferred to the supplementary material, and the R implementations of the proposed methods are publicly available through the author’s GitHub repository.¹

1.4 Notation

We fix the notation, which is used throughout the paper. Our methodology is founded on a Hilbert space framework. We use $\mathbb{H}, \mathbb{H}', \mathbb{H}''$ to represent infinite-dimensional separable Hilbert spaces; this distinction will be needed only when data and parameters spaces are different. As an example, we mainly work on the space $L^2([0, 1])$ of all square-integrable real-valued functions on $[0, 1]$, where the inner product there is defined as $\langle f, g \rangle \equiv \int_0^1 f(t)g(t)dt$ for $f, g \in L^2([0, 1])$ and induces norm $\|\cdot\|$. For univariate functions f_1, \dots, f_p on some common domain E , $\mathbf{f} = (f_1, \dots, f_p)^\top : E \rightarrow \mathbb{R}^p$ is the multivariate function defined by $\mathbf{f}(t) = (f_1(t), \dots, f_p(t))^\top$ for $t \in E$. In particular, if $\{f_1, \dots, f_p\} \subseteq \mathbb{H} = L^2([0, 1])$, then $\mathbf{f} = (f_1, \dots, f_p)^\top$ resides in another separable Hilbert space $\mathbb{H}' = \{L^2([0, 1])\}^p$. For x in a Hilbert space \mathbb{H} , $x^{\otimes 2} = x \otimes x$ is a shorthand expression to denote the squared tensor product operator of x on \mathbb{H} , defined by $x^{\otimes 2}(f) = \langle x, f \rangle x$ for $f \in \mathbb{H}$.

For a Hilbert space \mathbb{H} , $\mathcal{P}(\mathbb{H})$ stands for the set of all probability distributions on \mathbb{H} . Let π

¹<https://github.com/luckyhm1928>

denote the Prohorov metric on the space $\mathcal{P}(\mathbb{H})$ of probability measures on \mathbb{H} (cf. Billingsley, 1999, Section 5). It is useful to recall that π characterizes the weak convergence in $\mathcal{P}(\mathbb{H})$. We reserve P to denote the distributions of the statistics or limiting random element, while Q is used for a generic notation for probability distributions. The set of all continuous real-valued functions is denoted by $C([0, 1])$ equipped with supremum norm $\|\cdot\|_{\text{sup}}$ defined as $\|f\|_{\text{sup}} \equiv \sup_{t \in [0, 1]} |f(t)|$ for $f \in C([0, 1])$. Also, for a probability distribution Q on $C([0, 1])$, a random element $Z \sim Q$, and each $t \in [0, 1]$, we write Q_t for denoting the probability distribution of $Z(t)$.

2 Depth-based inference for functional parameters

Here, we describe the depth statistic in a general Hilbert space framework. We suppose data observations \mathcal{D}_n including functional data valued in \mathbb{H} are given for statistical inference for functional parameter $\theta \in \mathbb{H}'$. Here, \mathbf{n} stands for the collection of all sample sizes, as we may observe multiple samples; $\mathbf{n} = n$ for one-sample cases. With estimator $\hat{\theta}$ for θ , we may construct a functional statistic $T_n \equiv A_n(\hat{\theta} - \theta_0)$ for testing $H_0 : \theta = \theta_0$ for some $\theta_0 \in \mathbb{H}'$. Here, $A_n : \mathbb{H}' \rightarrow \mathbb{H}''$ is a bounded linear operator from \mathbb{H}' to a possibly different separable Hilbert space \mathbb{H}'' with minimum eigenvalue $\lambda_{A, \min, n}$ being positive but diverging. This operator represents a normalizing or scaling term. While there are various cases where $\mathbb{H}, \mathbb{H}', \mathbb{H}''$ are different, sample sizes are multiple, and scaling could be an operator (cf. Section 3), we describe our proposal assuming $\mathbb{H} = \mathbb{H}' = \mathbb{H}''$, $\mathbf{n} = n$, and scalar scaling, since the argument will not lose generality.

Let P_n denote the (true) sampling distribution P_n of T_n under H_0 , i.e., $P_n(A) = \mathbf{P}(T_n \in A | H_0)$ for a Borel set A in \mathbb{H} . Consider a depth function $D(\cdot; P_n)$ on \mathbb{H} with respect to P_n of T_n . Then, to test $H_0 : \theta = \theta_0$, we propose using the *depth statistic* defined by

$$DT_n \equiv D(T_n; P_n). \tag{1}$$

We note that small values of DT_n give evidence against H_0 .

While the depth statistic in (1) is flexible, it requires finding the sampling distribution P_n and computing the distribution F_n of the depth statistic, which may not have explicit forms. Here, F_n stands for the cumulative distribution function (CDF) of DT_n under H_0 , i.e., $F_n(u) = \mathbf{P}(DT_n \leq u | H_0)$ for $u \in \mathbb{R}$. For this, we estimate F_n by employing a resampling method. Suppose we have a consistent resampling method at hand so that we construct resampling statistic $T_n^* \equiv A_n(\hat{\theta}^* - \hat{\theta})$ with its (resampling) distribution \hat{P}_n under H_0 . The resampling depth statistic is given by

$$DT_n^* \equiv D(T_n^*; \hat{P}_n) \tag{2}$$

with CDF $\widehat{F}_n \equiv \mathbf{P}^*(DT_n^* \leq \cdot | H_0)$ under H_0 .

We will show that, given the consistency of the sampling and resampling distributions and some continuity properties of the depth, the resampling depth statistic distribution \widehat{F}_n consistently estimates its original version F_n . Before stating the theorem, we list the technical assumptions.

(C1) There exists $P \in \mathcal{P}(\mathbb{H})$ such that $\pi(P_n, P) \rightarrow 0$ as $n \rightarrow \infty$;

(C2) $\pi(\widehat{P}_n, P_n) \xrightarrow{\mathbf{P}} 0$ as $n \rightarrow \infty$;

(C3) for a sequence $\{x_n\}$ in \mathbb{H} and $x \in \mathbb{H}$ such that $x_n \rightarrow x \in \mathbb{H}$, $\{D(x_n; Q)\}$ converges to $D(x; Q)$ uniformly over $Q \in \mathcal{P}(\mathbb{H})$, i.e., $\sup_{Q \in \mathcal{P}(\mathbb{H})} |D(x_n; Q) - D(x; Q)| \rightarrow 0$;

(C4) for a sequence $\{Q_n\}$ in $\mathcal{P}(\mathbb{H})$ and $Q \in \mathbb{H}$ such that $\pi(Q_n, Q) \rightarrow 0$, $\{D(x; Q_n)\}$ converges to $D(x; Q)$ uniformly over $x \in \mathbb{H}$, i.e., $\sup_{x \in \mathbb{H}} |D(x; Q_n) - D(x; Q)| \rightarrow 0$; and

(C5) for $T \sim P$, the cumulative distribution function of the random variable $D(T; P)$ is continuous.

Condition (C1) means that the sampling distribution P_n weakly converges to some limiting distribution $P \in \mathcal{P}(\mathbb{H})$, while in Condition (C2), the resampling distribution \widehat{P}_n consistently estimates P_n , implying its weak convergence to P . In Conditions (C3)–(C5), we require the depth function to be (uniformly) continuous in either the element $x \in \mathbb{H}$ and the probability measure $P \in \mathcal{P}(\mathbb{H})$. We remark that Condition (C5), though mild, may fail for degenerate functional depths (Gijbels and Nagy, 2017). To assure practical relevance of these technical conditions, we will provide concrete examples that satisfy Conditions (C1)–(C2) in Section 3 and Conditions (C3)–(C5) in Section 4, respectively. Our main theoretical result is given below, while the proof is deferred to Section A.1 of the supplement.

Theorem 1. *Suppose that Conditions (C1)–(C5) hold. Then, the distribution \widehat{F}_n of the resampling depth statistic DT_n^* consistently estimates the distribution F_n of the original depth statistic DT_n in the sense that*

$$\sup_{u \in \mathbb{R}} |\widehat{F}_n(u) - F_n(u)| \xrightarrow{\mathbf{P}} 0.$$

In practice, like other resampling-based methods, we approximate the resampling depth statistic distribution \widehat{F}_n using Monte Carlo iterations. The procedure is summarized as follows and it can be applied to a general situation provided that the resampling consistency is guaranteed. For $b = 1, \dots, B$, we draw resampled data $\mathcal{D}_{b,n}$ to compute the resampling statistic $T_{b,n}^*$. Then, \widehat{F}_n is approximated by

$$\widetilde{F}_n(u) = \widetilde{F}_{n,B}(u) \equiv B^{-1} \sum_{b=1}^B \mathbb{I}(D(T_{b,n}^*; \widetilde{P}_n) \leq u), \quad u \in \mathbb{R}, \quad (3)$$

where $\tilde{P}_n = \tilde{P}_{n,B}$ denotes the empirical distribution of the resampled statistics $\mathcal{T}_{B,n} \equiv \{T_{b,n}^*\}_{b=1}^B$.

Depth p-value A natural application of the proposed depth statistic is the *depth p-value* defined by $\pi_n \equiv F_n(DT_n)$. With $\widehat{DT}_n \equiv D(T_n; \widehat{P}_n)$, the resampling depth p-value $\hat{\pi}_n$ is then defined by

$$\hat{\pi}_n \equiv \widehat{F}_n(\widehat{DT}_n). \quad (4)$$

This resampling depth p-value is indeed valid because it asymptotically follows the standard uniform distribution $U(0, 1)$ as asserted in [Theorem 2](#). The result is a direct consequence of [Theorem 1](#), whose proof is given in [Section A.1](#) of the supplement.

Theorem 2. *Suppose that Conditions (C1)–(C5) hold. The resampling depth p-value $\hat{\pi}_n$ in (4) converges in distribution to the standard uniform distribution, i.e., $\hat{\pi}_n \xrightarrow{d} U(0, 1)$.*

Using the approximate distribution \tilde{F}_n in (3), the estimated depth p-value $\hat{\pi}_n$ by a resampling method is approximated via Monte Carlo approximation by

$$\tilde{\pi}_n = \tilde{\pi}_{n,B} \equiv \tilde{F}_n(\widetilde{DT}_n), \quad (5)$$

where $\widetilde{DT}_n \equiv D(T_n; \tilde{P}_n)$. We use the approximate p-value in (5) for testing the null hypothesis $H_0 : \theta = \theta_0$. Namely, if the p-value $\tilde{\pi}_n$ is no bigger than the significance level, then we reject H_0 .

Remark 1. One could use the proposed depth statistic to construct a confidence region for infinite-dimensional parameter θ , e.g., by inverting the test for $H_0 : \theta = \theta_0$ ([Casella and Berger, 2002](#), Section 9.2.1). The subsequent confidence region may be given by

$$\widehat{C}_n \equiv \{f \in \mathbb{H}' : D(A_n(\hat{\theta} - f); \widehat{P}_n) \geq \widehat{F}_n^{-1}(\alpha)\},$$

where its $1 - \alpha$ asymptotic coverage can be derived from [Theorem 1](#) under Conditions (C1)–(C5) (cf. [Yeon and Kokoszka, 2026+](#), Lemma F.7). Nevertheless, we do not pursue these tools as using them for testing $H_0 : \theta = \theta_0$ is equivalent to testing H_0 with the depth p-value in (4).

3 Inference problems for functional data

As established in [Theorem 1](#), the proposed depth statistic demonstrates broad applicability. Among the numerous examples of functional parameter inference problems to which it may be applied, we elaborate on several representative cases below.

Example 1 (Functional ANOVA). Let $\{X_{ki}\}_{i=1}^{n_k}$, $k = 1, \dots, K$, be $K \in \mathbb{N}$ independent random samples that take values in a Hilbert space \mathbb{H} , where $\mathbf{n} = (n_1, \dots, n_K)$ denotes the collection of all sample sizes. For each $k = 1, \dots, K$, we consider the following setup. Suppose that these functional observations have finite second moment, i.e., $\mathbb{E}[\|X_{k1}\|^2] < \infty$, and define their mean functions and covariance operators as $\mu_k \equiv \mathbb{E}[X_{k1}]$ and $\Gamma_k \equiv \text{var}[X_{k1}] = \mathbb{E}[(X_{k1} - \mu_k)^{\otimes 2}]$. We write $\bar{X}_k \equiv n_k^{-1} \sum_{i=1}^{n_k} X_{ki}$ and $\hat{\Gamma}_k \equiv n_k^{-1} \sum_{i=1}^{n_k} (X_{ki} - \bar{X}_k)^{\otimes 2}$ to denote the sample mean and sample covariance of group k , respectively. Furthermore, ϕ_{kj} and $\hat{\phi}_{kj}$ denotes the j -th eigenfunctions of Γ_k and $\hat{\Gamma}_k$, respectively.

- (a) *Two-sample tests.* We first consider the case with $K = 2$ and define $a_{\text{two}, \mathbf{n}} = (n_1^{-1} + n_2^{-1})^{-1/2}$. The null hypotheses and corresponding functional statistics are summarized in Table 1 depending on the types of the tests. These problems have been widely studied by Dette et al. (2020), Fremdt et al. (2014), Horváth et al. (2013) for mean, Panaretos et al. (2010), Pigoli et al. (2014) for covariance, and Aue et al. (2023), Benko et al. (2009), Zhang and Shao (2015) for eigenfunctions, to name a few.

Table 1: The null hypotheses and test statistics for different functional two-sample tests.

Tests	Null hypotheses	Test statistics
Mean	$\mu_1 = \mu_2$	$a_{\text{two}, \mathbf{n}}(\bar{X}_1 - \bar{X}_2)$
Covariance	$\Gamma_1 = \Gamma_2$	$a_{\text{two}, \mathbf{n}}(\hat{\Gamma}_1 - \hat{\Gamma}_2)$
Eigenfunction	$\phi_{1j} = \phi_{2j}$	$a_{\text{two}, \mathbf{n}}(\hat{\phi}_{1j} - \hat{\phi}_{2j})$

- (b) *Test for equality between several means.* For general K , we are interested in testing the equality between several means stated as $H_{K, \text{mean}, 0} : \mu_1 = \dots = \mu_K$. We re-parametrize this problem with

$$\boldsymbol{\theta} = (\mu_2 - \mu_1, \dots, \mu_K - \mu_1)^\top$$

so that $H_{K, \text{mean}, 0}$ is equivalent to the statement that $\boldsymbol{\theta} = \mathbf{0}$. Then, we consider the multivariate functional statistic

$$T_{K, \text{mean}, \mathbf{n}} \equiv (a_{2\mathbf{n}}(\bar{X}_2 - \bar{X}_1), \dots, a_{K\mathbf{n}}(\bar{X}_K - \bar{X}_1))^\top$$

with $a_{k\mathbf{n}} = (n_k^{-1} + n_1^{-1})^{-1/2}$ for $k = 2, \dots, K$. Other parametrizations are possible such as $\boldsymbol{\theta} = (\mu_1 - \mu_K, \dots, \mu_{K-1} - \mu_K)^\top$. Some selective studies about this problem include Cuevas et al. (2004), Górecki and Smaga (2015), Paparoditis and Sapatinas (2016), Zhang and Liang (2014), Zhang et al. (2019).

Example 2 (Functional regression). We illustrate the wide applicability of the proposed depth statistic with several functional regression models with functional responses. Below,

let $\{Y_i\}_{i=1}^n$ and $\{\varepsilon_i\}_{i=1}^n$ respectively denote functional responses and functional errors that take values in $\mathbb{H} = L^2([0, 1])$, with sample size $\mathbf{n} = n$, and $\alpha \in \mathbb{H}$ represent the intercept function, while the structures of regressors can be different depending on models.

(a) *Functional concurrent regression and function-on-scalar regression:*

$$Y_i(t) = \alpha(t) + \mathbf{x}_i(t)^\top \boldsymbol{\beta}(t) + \varepsilon_i(t), \quad t \in [0, 1], \quad i = 1, \dots, n,$$

where \mathbf{x}_i is a p -dimensional functional regressor with $\mathbf{x}_i(t) = (x_{i1}(t), \dots, x_{ip}(t))^\top$ for each $t \in [0, 1]$. With $\boldsymbol{\beta}(t) = (\beta_1(t), \dots, \beta_p(t))^\top$ for $t \in [0, 1]$, we write $\boldsymbol{\beta}_1$ for the later part of the coefficient function $\boldsymbol{\beta}$ such that $\boldsymbol{\beta}_1(t) \equiv (\beta_{q+1}(t), \dots, \beta_p(t))^\top$ for each $t \in [0, 1]$. We may be interested in a partial test $H_0 : \boldsymbol{\beta}_1 = \mathbf{0}$. For this testing, we may adopt the classical least squares estimator pointwise. To explain, we define the following quantities for each $t \in [0, 1]$:

$$\mathbf{X}_0(t) \equiv [x_{ij}(t)]_{1 \leq i \leq n, 0 \leq j \leq q}, \quad \mathbf{X}_1(t) \equiv [x_{ij}(t)]_{1 \leq i \leq n, q+1 \leq j \leq p}, \quad \mathbf{X}(t) = \begin{bmatrix} \mathbf{X}_0(t) & \mathbf{X}_1(t) \end{bmatrix},$$

where $x_{i0}(t) = 1$, along with projection matrix $\Pi_{\mathbf{X}_0(t)} \equiv \mathbf{X}_0(t) \{ \mathbf{X}_0(t)^\top \mathbf{X}_0(t) \}^{-1} \mathbf{X}_0(t)^\top$ and the orthogonal complement data matrix $\mathbf{X}_{1|0}(t) \equiv \mathbf{X}_1(t) - \Pi_{\mathbf{X}_0(t)} \mathbf{X}_1(t)$. Then, the (pointwise) least squares estimator $\hat{\boldsymbol{\beta}}_1$ for $\boldsymbol{\beta}_1$ is defined by

$$\hat{\boldsymbol{\beta}}_1(t) \equiv \{ \mathbf{X}_{1|0}(t)^\top \mathbf{X}_{1|0}(t) \}^{-1} \mathbf{X}_{1|0}(t)^\top \mathbf{Y}(t), \quad t \in [0, 1].$$

The multivariate functional statistic for $H_0 : \boldsymbol{\beta}_1 = \mathbf{0}$ is then $T_{\text{fcr},n} \equiv \sqrt{n} \hat{\boldsymbol{\beta}}_1$. This framework is studied by Ghosal and Maity (2022), Wang et al. (2018). In particular, it includes (i) testing in function-on-scalar regression models (Chang et al., 2017, Shen and Faraway, 2004, Zhang, 2011, Zhang and Chen, 2007) when we consider constant functions for all regressors $\{\mathbf{x}_i\}_{i=1}^n$, (ii) functional ANOVA setups for comparing several means as in Example 1(b) with suitable design matrix, and (iii) hence two-sample mean tests described in Example 1(a).

(b) *Function-on-function regression (FoFR):*

$$Y_i = \alpha + \mathbf{B}X_i + \varepsilon_i, \quad i = 1, \dots, n, \tag{6}$$

where $\mathbf{B} : \mathbb{H} \rightarrow \mathbb{H}$ is a bounded linear operator on \mathbb{H} and X_i is a random element that take values in \mathbb{H} . Although direct inference for \mathbf{B} may not be feasible since CLT for \mathbf{B} itself may not exist (Crambes and Mas, 2013), we can conduct inference for mean response $\mu(X_0) \equiv \alpha + \mathbf{B}X_0$ at a new functional regressor X_0 . Namely, we may be interested in testing whether the mean response $\mu(X_0)$ at X_0 is equal to the global mean $\mathbf{E}[Y]$, which can be represented by the null hypothesis $H_0 : \mu(X_0) = \mathbf{E}[Y]$ (cf.

Yeon, 2026+). This is equivalent to the statement $\theta \equiv \mathbb{B}(X_0 - \mathbb{E}[X]) = 0$. A functional statistic is then $T_{\text{fofr},n} \equiv \sqrt{n/\hat{s}}\hat{B}(X_0 - \bar{X})$ with suitable estimator \hat{B} for B and scaling \hat{s} . This problem is treated by Yeon (2026+) with L^2 norm and Dette and Tang (2024) with sup norm. See Section 3.2 for more details about the test statistic developed by Yeon (2026+).

In what follows, we focus on the two-sample functional mean tests in Example 1(a) and the mean response inference for FoFR in Example 2(b), whose bootstrap procedures are described in Sections 3.1–3.2, respectively.

3.1 Two-sample functional mean tests

We explain a bootstrap method for two-sample inference for functional data. Following the setup in Example 1(a), we consider the two-sample test statistic defined by

$$T_{\text{two},n} = \sqrt{\frac{n_1 n_2}{n_1 + n_2}} (\bar{X}_1 - \bar{X}_2) \quad (7)$$

with $\mathbf{n} \equiv (n_1, n_2)$. For the resampling implementation of our depth-based two-sample test, we adopt the following residual-type bootstrap method; see Benko et al. (2009), Dette et al. (2020), Paparoditis and Sapatinas (2016) for other bootstrap two-sample functional mean tests. With the pooled sample mean $\bar{X} \equiv (n_1 + n_2)^{-1}(n_1 \bar{X}_1 + n_2 \bar{X}_2)$, for each $k = 1, 2$, the bootstrap resamples are defined by $X_{ki}^* \equiv \bar{X} + \varepsilon_{ki}^*$, where bootstrap errors $\varepsilon_{k1}^*, \dots, \varepsilon_{kn_k}^*$ are iid uniform draws from the (centered) residuals $\{\hat{\varepsilon}_{ki} \equiv X_{ki} - \bar{X}_k\}_{i=1}^{n_k}$. The bootstrap statistic is then defined by

$$T_{\text{two},n}^* \equiv \sqrt{\frac{n_1 n_2}{n_1 + n_2}} (\bar{X}_1^* - \bar{X}_2^*), \quad (8)$$

where $\bar{X}_k^* \equiv n_k^{-1} \sum_{i=1}^{n_k} X_{ki}^*$ for $k = 1, 2$. For completeness, we provide the asymptotic and bootstrap results for this functional two-sample framework along with its proof (Section A.2 of the supplement), as we have not found an exact reference.

Theorem 3. *Suppose that $n_1 \rightarrow \infty$ and $n_2 \rightarrow \infty$ along with $n_1/(n_1 + n_2) \rightarrow \zeta \in (0, 1)$. We further assume that each random function X_{ki} has finite second moment with covariance operator Γ_k . By denoting $P_{\text{two},n}$ and $\hat{P}_{\text{two},n}$ for the distributions of $T_{\text{two},n}$ in (7) and $T_{\text{two},n}^*$ in (8), respectively, we have the following:*

- (a) $\pi(P_{\text{two},n}, P_{\text{two},\zeta}) \rightarrow 0$, where $P_{\text{two},\zeta}$ represents the Gaussian distribution on \mathbb{H} with mean zero and covariance $(1 - \zeta)\Gamma_1 + \zeta\Gamma_2$; and
- (b) $\pi(\hat{P}_{\text{two},n}, P_{\text{two},n}) \rightarrow 0$ almost surely.

3.2 FoFR mean response inference

We illustrate the depth statistic in the FoFR setting described in [Example 2\(b\)](#). For this, we follow the estimation and bootstrap inference procedure developed in [Yeon \(2026+\)](#). We observe n functional response-regressor pairs $\{(Y_i, X_i)\}_{i=1}^n$ from the FoFR model in (6), and a new functional predictor $X_0 \stackrel{d}{=} X_1$ is given. The covariance operator of $\{X_i\}_{i=1}^n$ and the cross-covariance operator between $\{Y_i\}_{i=1}^n$ and $\{X_i\}_{i=1}^n$ are respectively given by

$$\begin{aligned}\widehat{\Gamma} &\equiv n^{-1} \sum_{i=1}^n (X_i - \bar{X})^{\otimes 2}, \\ \widehat{\Delta} &\equiv n^{-1} \sum_{i=1}^n \{(Y_i - \bar{Y}) \otimes (X_i - \bar{X})\},\end{aligned}$$

where $\bar{X} \equiv n^{-1} \sum_{i=1}^n X_i$ and $\bar{Y} \equiv n^{-1} \sum_{i=1}^n Y_i$ represent the sample means. The covariance operator $\widehat{\Gamma}$ admits spectral decomposition ([Hsing and Eubank, 2015](#), Chapter 4) as $\widehat{\Gamma} = \sum_{j=1}^n \hat{\gamma}_j (\hat{\phi}_j \otimes \hat{\phi}_j)$, where $(\hat{\gamma}_j, \hat{\phi}_j)$ is the j -th eigenvalue-eigenfunction pair of $\widehat{\Gamma}$. To estimate the slope estimator \mathbf{B} , we regularize the inversion of $\widehat{\Gamma}$ by truncating it up to the truncation level $J = J_n$. Namely, with a truncated inverse covariance operator $\widehat{\Gamma}_J^{-1} \equiv \sum_{j=1}^J \hat{\gamma}_j^{-1} (\hat{\phi}_j \otimes \hat{\phi}_j)$, the functional principal component regression (FPCR) estimator $\widehat{\mathbf{B}}_J$ for \mathbf{B} is defined by

$$\widehat{\mathbf{B}}_J \equiv \widehat{\Delta} \widehat{\Gamma}_J^{-1}. \quad (9)$$

Upon scaling, the test statistic for $H_0 : \mu(X_0) = \mathbf{E}[Y]$ is then defined by

$$T_{\text{fofr},n}(X_0) \equiv \sqrt{\frac{n}{\hat{\tau}_J(X_0)}} \widehat{\mathbf{B}}_J (X_0 - \bar{X}), \quad (10)$$

where the scaling term is defined by

$$\hat{\tau}_J(x) \equiv \sum_{j=1}^J \hat{\gamma}_j^{-1} \langle x - \bar{X}, \hat{\phi}_j \rangle^2, \quad x \in \mathbb{H}.$$

The following residual bootstrap is shown to be valid to approximate the distribution of $T_n(X_0)$ in (10). We first compute the residuals as $\hat{\varepsilon}_{i,J_{\text{res}}} \equiv Y_i - \bar{Y} - \widehat{\mathbf{B}}_{J_{\text{res}}}(X_i - \bar{X})$ for additional truncation level $J_{\text{res}} = J_{\text{res},n}$ with $\widehat{\mathbf{B}}_{J_{\text{res}}} \equiv \widehat{\Delta} \widehat{\Gamma}_{J_{\text{res}}}^{-1}$. Then, the bootstrap errors $\{\varepsilon_i^*\}_{i=1}^n$ are drawn uniformly from $\{\varepsilon_{i,K}\}_{i=1}^n$ with replacement and we compute the bootstrap responses akin to (6) as

$$Y_i^* \equiv \bar{Y} + \widehat{\mathbf{B}}_{J_{\text{cen}}}(X_i - \bar{X}) + \varepsilon_i^*, \quad i = 1, \dots, n,$$

where $\widehat{\mathbf{B}}_{J_{\text{cen}}} \equiv \widehat{\Delta} \widehat{\Gamma}_{J_{\text{cen}}}^{-1}$ plays a role of the true parameter in the bootstrap world with another extra truncation $J_{\text{cen}} = J_{\text{cen},n}$. The bootstrap slope estimator $\widehat{\mathbf{B}}_J^*$ is constructed analogously

to (9) as

$$\widehat{\mathbf{B}}_J^* \equiv \widehat{\Delta}^* \widehat{\Gamma}_J^{-1},$$

where $\widehat{\Delta}^* \equiv n^{-1} \sum_{i=1}^n \{(Y_i^* - \bar{Y}^*) \otimes (X_i - \bar{X})\}$ with $\bar{Y}^* \equiv n^{-1} \sum_{i=1}^n Y_i^*$. The bootstrap test statistic is then defined by

$$T_{\text{fofr},n}^*(X_0) \equiv \sqrt{\frac{n}{\widehat{\tau}_J(X_0)}} (\widehat{\mathbf{B}}_J^* - \widehat{\mathbf{B}}_{J_{\text{cen}}})(X_0 - \bar{X}). \quad (11)$$

Regarding the mean response inference in this function-on-function regression framework, the following theorem is established by [Yeon \(2026+\)](#).

Theorem 4. *Write $P_{\text{fofr},n}$ and $\widehat{P}_{\text{fofr},n}$ for the distributions of $T_{\text{fofr},n}(X_0)$ in (10) and $T_{\text{fofr},n}^*(X_0)$ in (11), respectively. Under the assumptions stated in [Section A.5](#) of the supplement, we have the following:*

- (a) $\pi(P_{\text{fofr},n}, P_{\text{fofr},\Sigma}) \rightarrow 0$, where $P_{\text{fofr},\Sigma}$ denotes the Gaussian random function on \mathbb{H} with mean zero 0 and covariance operator $\Sigma \equiv \mathbf{E}[\varepsilon \otimes \varepsilon | X]$; and
- (b) $\pi(\widehat{P}_{\text{fofr},n}, P_{\text{fofr},n}) \xrightarrow{\mathbb{P}} 0$.

4 Functional depth

We review four representative functional depths among others: kernel, regularized halfspace, integrated, and infimal, depths. The former two are defined on a general separable Hilbert space \mathbb{H} , hence incorporating any Hilbertian random elements (cf. [Jeon and Park, 2020](#)). The latter two are defined on $C([0, 1])$ and successfully extended to multivariate functional data possibly on multivariate domain. We first introduce the kernel depth and establish that Conditions (C3)–(C5) hold for it. Although it is unclear that Conditions (C3)–(C4) are satisfied for the second depth and the last two depths are defined on a Banach space, we will shortly review them and include the corresponding depth statistics in our numerical studies for a broader comparison.

4.1 Kernel depth

We first introduce a functional depth which we call the kernel depth ([Cuevas et al., 2006](#)). Let $K : [0, \infty) \rightarrow [0, \infty)$ be a continuous and non-increasing function with $K(0) > 0$ and $\lim_{t \rightarrow \infty} K(t) = 0$, which we call a kernel (function). Popular kernels include the Gaussian kernel given by $K(t) = e^{-t^2/2}$ for $t \in [0, \infty)$. The *kernel depth* (KD) of $x \in \mathbb{H}$ (induced by

K) with respect to a probability measure Q on \mathbb{H} is defined by

$$D_K(x; Q) = \mathbf{E}[K(\|x - X\|)] \quad (12)$$

where $X \sim Q$. Traditionally, D_K has been called *h-mode depth*, since its practical version involves a bandwidth $h \in (0, \infty)$. Namely, upon defining a normalized kernel K_h as $K_h(u) = h^{-1}K(h^{-1}u)$ for $u \in [0, \infty)$, then the sample KD of $x \in \mathbb{H}$ is defined by

$$D_{K_h}(x; \widehat{Q}_n) = (nh)^{-1} \sum_{i=1}^n K(h^{-1}\|x - X_i\|), \quad (13)$$

where \widehat{Q}_n stands for the empirical distribution defined through $\{X_i\}_{i=1}^n$. Here, the bandwidth h can be data-adaptively selected. For example, for $u \in (0, 1)$, we may take u -th quantile of the observed distances $\{\|X_{i'} - X_i\| : i \neq i'\}$, where a KD with smaller u tends to be sensitive to shapes of the functional observations. In addition to its computational scalability, more advantages of the KD D_K are recently found: it can characterize a distribution on \mathbb{H} and exhibit uniform consistency over the entire function space \mathbb{H} with a suitable kernel. While we direct readers to [Wynne and Nagy \(2025\)](#) for a comprehensive review of the KD, we provide some useful results for our methodology.

Theorem 5. *Let $K : [0, \infty) \rightarrow \mathbb{R}$ be a bounded and continuous function. Regarding the KD $D_K(x; Q)$ for $x \in \mathbb{H}$ and $Q \in \mathcal{P}(\mathbb{H})$ defined in Equation (12), we have the following two continuity properties.*

- (a) *The map $x \mapsto D_K(x; Q)$ is continuous uniformly over $Q \in \mathcal{P}(\mathbb{H})$ in the sense that, for a sequence $\{x_n\}$ in \mathbb{H} and $x \in \mathbb{H}$, as $n \rightarrow \infty$, if $x_n \rightarrow x$, then we have*

$$\sup_{Q \in \mathcal{P}(\mathbb{H})} |D_K(x_n; Q) - D_K(x; Q)| \rightarrow 0.$$

- (b) *The map $Q \mapsto D_K(\cdot; Q)$ is continuous uniformly over $x \in \mathbb{H}$ in the sense that, for a sequence $\{Q_n\}$ in $\mathcal{P}(\mathbb{H})$ and $Q \in \mathcal{P}(\mathbb{H})$, as $n \rightarrow \infty$, if Q_n weakly converges to Q , then we have*

$$\sup_{x \in \mathbb{H}} |D_K(x; Q_n) - D_K(x; Q)| \rightarrow 0.$$

The proof of [Theorem 5](#) is given in [Section A.3](#) of the supplement. [Theorem 5](#) basically indicates that the KD satisfies Conditions (C3)–(C4). These two results are not clearly established in the literature, although a uniform consistency by the empirical distribution is given in [Wynne and Nagy \(2025, Theorem 5\)](#). It is important to note that the KD is useful especially for functional (infinite-dimensional) data, because such convergence results

of functional depths uniform on an entire space have been rarely found. In addition, the continuity of the KD in probability measures is closely related to that in the so-called maximum mean discrepancy in Machine Learning literature (cf. [Simon-Gabriel et al., 2023](#)). While we do not attempt to thoroughly study this direction, we refer to [Wynne and Nagy \(2025\)](#) for more details about this relationship.

We close this section by providing an important example where the KD additionally satisfies Condition [\(C5\)](#). To summarize, using KD, Theorems [1–2](#) hold (i.e., the depth statistic is valid) for the inference problems in Sections [3.1–3.2](#).

Example 3. Let $P \in \mathcal{P}(\mathbb{H})$ be the Gaussian with mean element $0 \in \mathbb{H}$ and a covariance operator $\Sigma : \mathbb{H} \rightarrow \mathbb{H}$. Then, by [Wynne and Nagy \(2025, Example 1\)](#), the kernel depth of $x \in \mathbb{H}$ with respect to P is explicitly written as

$$D_K(x; P) = \left\{ \prod_{j=1}^{\infty} (1 + \sigma_j) \right\}^{-1/2} \exp \left[-\frac{1}{2} \sum_{j=1}^{\infty} \frac{\langle x, \psi_j \rangle^2}{1 + \sigma_j} \right],$$

where (σ_j, ψ_j) denotes the j -th eigenvalue-eigenfunction pair of Σ . Let $T \sim P$, which is the case in most asymptotic distributional theories. Then, since $\{\sigma_j^{-1/2} \langle T, \psi_j \rangle\}_{j=1}^{\infty}$ is a sequence of independent standard normal variables, the random variable

$$V \equiv \sum_{j=1}^{\infty} \frac{\langle T, \psi_j \rangle^2}{1 + \sigma_j} \stackrel{d}{=} \sum_{j=1}^{\infty} \frac{\sigma_j}{1 + \sigma_j} (\sigma_j^{-1/2} \langle T, \psi_j \rangle)^2$$

is a infinite mixture of independent χ^2 random variables with one degree of freedom, which is hence continuous. Note that $\mathbf{P}(0 < V < \infty) = 1$, implying that $\mathbf{P}(D_K(T; P) > 0) = 1$. Since the map $\mathbb{R} \ni a \mapsto e^{-a/2} \in \mathbb{R}$ is one-to-one, $D_K(T; P)$ is a continuous random variable.

4.2 Regularized halfspace depth

It is well-known that a naive extension of the celebrated Tukey’s halfspace depth ([Tukey, 1975](#)) can be degenerate in an infinite-dimensional space ([Dutta et al., 2011](#)). To describe, we define the functional halfspace depth (FHD) $D_{\text{FHD}}(x; Q)$ of $x \in \mathbb{H}$ at $Q \in \mathcal{P}(\mathbb{H})$ as

$$D_{\text{FHD}}(x; Q) = \inf_{v \in \mathbb{H}: \|v\|=1} \mathbf{P}(\langle X - x, v \rangle \geq 0),$$

where $X \sim Q$. However, for example, when Q is Gaussian, the FHD is turned out to be degenerate as $\mathbf{P}(D_{\text{FHD}}(T; Q) = 0) = 1$ for $T \sim Q$ independent of X (cf. [Yeon et al., 2025](#)). In our context, unlike the KD (cf. [Example 3](#)), the FHD may not satisfy Condition [\(C5\)](#).

To address this degeneracy of the FHD, the regularized halfspace depth (RHD) was recently introduced by [Yeon et al. \(2025\)](#). This generalize the classical halfspace depth on the Euclidean space to a general Hilbert space by regularizing the dispersions of projections

in the projection direction set. Let $Q \in \mathcal{P}(\mathbb{H})$, $X \sim Q$ with $\mathbb{E}[\|X\|^2] < \infty$. We denote $\Gamma(Q) \equiv \mathbb{E}[(X - \mathbb{E}[X])^{\otimes 2}]$ for its covariance operator. To reduce computational burden due to spectral decomposition used in the original RHD, we suggest using the following modified version: for $Q \in \mathcal{P}(\mathbb{H})$ and $x \in \mathbb{H}$,

$$D_{\text{RHD},\lambda}(x; Q) \equiv \inf_{v \in \mathbb{H}: \|v\|=1, \|\Gamma(Q)^{1/2}v\| \geq \lambda} \mathbb{P}(\langle X - x, v \rangle \geq 0), \quad (14)$$

where $X \sim Q$. Here, $\Gamma(Q)^{1/2}$ stands for the square root operator of $\Gamma(Q)$; see [Hsing and Eubank \(2015\)](#) for general Hilbert space theory. Unlike the FHD exhibits degeneracy, the RHD is shown to be degenerate by [Yeon et al. \(2025\)](#), which ensures its practicality. For completeness, we provide a nondegeneracy result of the modified RHD (14) in [Section A.4](#) of the supplement. The random projection approach is adopted to approximate the sample RHD. Namely, we generate directions $\{v_m\}_{m=1}^M$ from $\{v \in \mathbb{H} : \|v\| = 1\}$, choose the u -th quantile of $\{\|\widehat{\Gamma}^{1/2}v_m\|\}_{m=1}^M$ to use the regularization λ , and compute the minimum of the empirical halfspace probabilities (cf. [Section B.1](#) of the supplement). Here, $\widehat{\Gamma} \equiv \Gamma(\widehat{Q}_n) = n^{-1} \sum_{i=1}^n (X_i - \bar{X})^{\otimes 2}$ denotes the sample covariance operator of the functional observations $\{X_i\}_{i=1}^n$, where $\bar{X} \equiv n^{-1} \sum_{i=1}^n X_i$ and \widehat{Q}_n denotes the empirical distribution of $\{X_i\}_{i=1}^n$. The quantile level u may provide different perspectives for statistical analysis; with smaller u , the resulting RHD considers more projection directions whose variances get smaller, and hence, becomes better sensitive to shapes of functional observations. The RHD then leads to developing an effective method to detect both magnitude and shape functional outliers.

4.3 Integrated and infimal depths

The last two functional depths for continuous functional data we introduce are integrated ([Fraiman and Muniz, 2001](#)) and infimal ([Mosler, 2013](#)) depths. These pointwise apply depth functions for univariate data and integrate these by taking either integral or infimum. To explain, let D_{uni} be a univariate depth function, such as halfspace ([Tukey, 1975](#)) or simplicial ([Liu, 1990](#)) depths, used for constructing functional depths. The integrated (ITD) and infimal (IFD) depths of $x \in C([0, 1])$ with respect to a probability distribution Q on $C([0, 1])$ are defined respectively by

$$D_{\text{ITD}}(x; Q) \equiv \int_0^1 D_{\text{uni}}(x(t); Q_t) dt,$$

$$D_{\text{IFD}}(x; Q) \equiv \inf_{t \in [0, 1]} D_{\text{uni}}(x(t); Q_t).$$

Their sample versions are defined by replacing the probability Q by its empirical counterpart \widehat{Q}_n . The implementation of both depth functions are well-developed in R package `ddalpha` ([Pokotylo et al., 2019](#)). While many other functional depths have been proposed, these

classical depth play benchmark roles in the literature. These depths can be extended to multivariate functional data defined possibly on multivariate domain (e.g., [Claeskens et al., 2014](#), [Qu et al., 2022](#)).

5 Numerical studies

All functional observations are generated based on the Karhunen–Loève expansion:

$$X = \mu + \sum_{j=1}^{J_{\text{true}}} \gamma_j^{-1/2} \xi_j \phi_j \quad (15)$$

for $\mu \in \mathbb{H}$. Here, the number $J_{\text{true}} = 20$ of true eigenfunctions are fixed for all simulation studies. The eigenvalues $\{\gamma_j\}_{j=1}^{J_{\text{true}}}$, eigenfunctions $\{\phi_j\}_{j=1}^{J_{\text{true}}}$, functional principal component (FPC) scores $\{\xi_j\}_{j=1}^{J_{\text{true}}}$ will vary depending on cases. The FPC scores are distributed as $\xi_j \stackrel{d}{=} \xi W_j$, where $W_j \stackrel{\text{iid}}{\sim} \mathbf{N}(0, 1)$ while the distribution of the latent variable ξ is given by either $\xi = 1$, $\xi \sim \mathbf{N}(0, 1)$, or $\xi \sim \text{Exp}(1) - 1$. We refer to these as N1-, NN-, NE-types of FPC scores, respectively. The former generates a Gaussian element with independent FPC scores, while in the latter two cases, the scores $\{\xi_j\}$ are dependent, which could lead to a difficult inference case (cf. [Yeon et al., 2023](#)). The eigenvalues are defined through their gaps $\gamma_j - \gamma_{j+1} = 2j^{-a}$ with $\gamma_1 \equiv 2 \sum_{j=1}^{\infty} j^{-a}$ and determined by the decay rate $a > 2$. For eigenfunctions, we consider subsets $\{\phi_{q,j}\}_{j=1}^{J_{\text{true}}}$ of four orthonormal systems for $q \in \{\text{tri, mono, cheb, spl}\}$ in $\mathbb{H} = L^2([0, 1])$: trigonometric functions, and orthonormalized monomials, (shifted) Chebyshev polynomials, and cubic splines functions. The details of the constructions of these basis functions are deferred to [Section B.2](#) of the supplement. All functions are evaluated 50 equi-distant grid in $[0, 1]$.

For depth statistics implementations based on IFD and ITD, we use well-implemented functions in the `dda` package in R ([Pokotylo et al., 2019](#)). The regularization λ for the RHD (14) and bandwidth for the KD in (13) are determined by quantile levels $u \in \{0.5, 0.4, 0.3, 0.2, 0.1, 0.01, 0.001\}$ as suggested by [Yeon et al. \(2025\)](#) and [Wynne and Nagy \(2025\)](#), respectively. We found that, in both sizes and power, $u = 0.1$ and $u = 0.001$ work best for the RHD statistic in two-sample and FoFR problems, respectively, while the KD statistic performs well with $u = 0.01$ in both problems. We only report the results from these quantile levels. In addition, to approximate the infimum in the RHD, we employ a random projection approach as in the original paper. Since the RHD may produce ties, we devise a new tie breaking algorithm and apply it to our numerical studies. The RHD implementations is further detailed in [Section B.1](#) of the supplement.

For the methods based on FPCs, where truncation may be involved, we consider truncation levels in $\{1, \dots, 20\}$. The truncation levels are chosen using fraction of variance explained (FVE), which is one of the most common approaches to select truncation level,

with threshold 0.85 (e.g, [Kokoszka and Reimherr, 2017](#), Section 12.2).

All tests are conducted at significance level 0.05. We conducted 1,000 Monte Carlo iterations to compute empirical rejection rates, which provide empirical sizes under a null hypothesis and empirical power under an alternative hypothesis. Bootstrap methods are implemented with 1,000 bootstrap resamples. Since the results are similar across scenarios for each problem, we only partially report them.

5.1 Two-sample functional mean tests

5.1.1 Simulation design

Two independent groups $\{X_{ki}\}_{i=1}^{n_k}$, $k = 1, 2$, of iid functional data are generated based on (15):

$$X_{ki} \equiv \mu_k + \sum_{j=1}^{J_{\text{true}}} \gamma_{k,j}^{1/2} \xi_{ki,j} \phi_{k,j}, \quad i = 1, \dots, n_k, \quad k = 1, 2.$$

The total sample sizes are given by $n \equiv n_1 + n_2 \in \{50, 200, 1000\}$, where the sample sizes of each group are equal as $n_1 = n_2 = n/2$. The FPC scores are distributed as $\xi_{ki,j} \stackrel{d}{=} \xi_j$, where ξ_j is from (15). We vary eigenvalues and eigenfunctions to consider different scenarios with equal and unequal covariance operators. Namely, when eigenvalues are equal, $\gamma_{k,j} - \gamma_{k,j+1} \equiv 2j^{-a_k}$ with $a_1 = a_2 = 2.5$; if eigenvalues differ across groups, $a_1 = 5$ and $a_2 = 2.5$. For scenarios with equal eigenfunctions, $\phi_{k,j} = \phi_{\text{tri},j}$ for both $k = 1, 2$, while when eigenfunctions are unequal, we set $\phi_{1,j} = \phi_{\text{mono},j}$ and $\phi_{2,j} = \phi_{\text{cheb},j}$. Similar constructions can be found in [Yeon and Kokoszka \(2026+\)](#), where the details are given in [Section B.2](#) of the supplement.

While the mean function μ_1 of the first group is set to be constant as $\mu_1 = 0 \in \mathbb{H} = L^2([0, 1])$, we consider seven functions with different shapes for the mean function of the second group under the strongest alternatives, inspired by outlier constructions considered in [Yeon et al. \(2025, Section 4.1\)](#). These respectively represent magnitude, jump, peak, linear, quadratic, cubic, and wiggle differences between mean functions. These are denoted by $\mu_{2,d}$ with index $d \in D_{\text{alter}} \equiv \{\text{Mag, Jump, Peak, Lin, Quad, Cub, Wig}\}$. We depict these seven curves in [Figure 2](#), while the detailed formulae are given in [Section B.3](#) of the supplement. It is worthwhile mentioning that such features cannot be considered in finite-dimensional cases. The true mean μ_2 of the second group is then defined by $\mu_2 = (1 - c)\mu_1 + c\mu_{2,d} = c\mu_{2,d}$ with $c \in \{0, 0.2, 0.4, 0.6, 0.8, 1\}$. Here, $c = 0$ renders the null hypothesis $H_0 : \mu_1 = \mu_2$, while the mean difference becomes larger as c increases.

5.1.2 Competing tests

In addition to the depth statistics based on ITD, IFD, RHD, and KD, we consider several different state-of-the-art competing methods for two-sample functional mean tests including

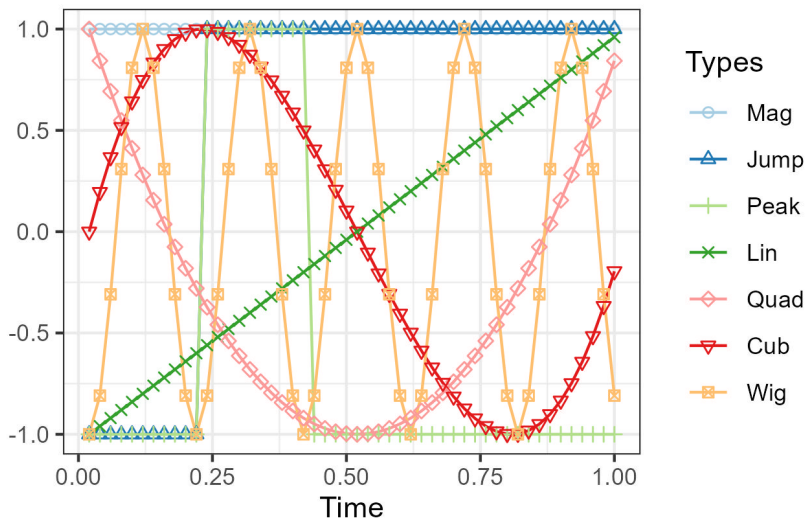


Figure 2: The curves with different shapes considered under strongest alternatives.

functional ANOVA approaches. The first group of competing methods are: the quadratic forms by Horváth et al. (2013), Sharghi Ghale-Joogh and Hosseini-Nasab (2018) (QuadInv and QuadMul, respectively); the L^2 statistic by Benko et al. (2009), Horváth et al. (2013), Paparoditis and Sapatinas (2016) (L2); the supremum statistic by Dette et al. (2020) (sup); the global (integrated) pointwise F statistic by Zhang and Liang (2014) (Fint); and the supremum pointwise F statistic by Zhang et al. (2019) (Fmax). Section B.4 of the supplement includes more details about the choice of truncation level for QuadInv and QuadMul. We calibrate the critical values for these test statistics using the same bootstrap method, the one described in Section 3.1. These are deserved to be called our main competitors as they are calibrated using the same bootstrap method and it will better show the effectiveness of the proposed depth statistic. Nevertheless, we also conduct the bootstrap for Fmax given in Zhang et al. (2019) (Fmaxb) for comparison, which is implemented by `fdANOVA::fanova.tests` in R with option `test="Fmaxb"`. It is important to note that the tests including Fmaxb and those described below may differ not only in their choice of test statistic but also in the resampling schemes used to approximate the sampling distributions. Consequently, although we include some comparison with these other tests, our main goal is a comparison between test statistics, not overall tests.

Beyond the aforementioned tests based on the bootstrap method in Section 3.1, other competitors include permutation tests based on random projections by Cuesta-Albertos and Febrero-Bande (2010) (TRP), basis function representation by Górecki and Smaga (2015) (FP), a functional version of the Hotelling's T^2 statistic by Pini et al. (2018) (HotSq), and graphical approach by Mrkvička et al. (2020) (GET). These are implemented in `fdANOVA` (Górecki and Smaga, 2019) (with options `test="TRP"` and `test="FP"`), `fdahotelling`,² and

²<https://github.com/astamm/fdahotelling>

GET (Myllymäki and s Mrkvička, 2024) packages, respectively.

In addition, we compare our depth statistics with confidence bands while treating the differences $\{Z_i \equiv X_{1i} - X_{2i}\}_{i=1}^{n/2}$ as one-sample. the naive pointwise t-test without adjusting for multiple testing (naive.t), and bands for mean functions proposed by Degras (2011) (Bs), Choi and Reimherr (2018) (BEc), and Liebl and Reimherr (2023) (FFSCB.t), which are implemented in `ffscb`³ package. In particular, regarding the fairness parameter for FFSCB.t, we use 1 as implemented in the package.

Finally, as a most recent method, we include high-dimensional bootstrap approach that is applicable to functional ANOVA problem, developed by Lin et al. (2023) and implemented in the package `hdanova`.⁴ Instead of the trigonometric functions $\{\phi_{\text{tri},j}\}$ onto which functional observations are projected in their method, we modify their function by considering the orthonormalized cubic spline functions $\{\phi_{\text{spl},j}\}$ for the basis choice. The tuning parameter for their partial standardization, we consider both zero and the default implementation. These are referred to as HANOVA0 and HDANOVA, respectively.

5.1.3 Empirical sizes and power

The empirical sizes of these 22 tests are given in Table 2, when $n = 50$ and the NN-type FPC scores are considered. Overall, including the depth statistics, many tests are able to keep the nominal level regardless of covariance differences. QuadInv, QuadMul, Fint, Fmax, TRP, Bs, naive.t provide conservative results. HotSq and FFSCB.t tend to fail to achieve the nominal level; as expected, HotSq is only applicable for equal covariance scenarios. FFSCB.t involves the fairness parameter, where the resulting power along with sizes becomes smaller as this parameter increases, which is observed by Liebl and Reimherr (2023).

We now turn to our attention to power analysis, which is more important in our simulation studies. The empirical rejection rates are provided in Figure 3 under the same scenario. Since the power curves overlap, which prevents visibility, we report the proposed depth statistics (red), our main competitors (QuadInv, L2, sup, Fint, Fmax, marked in blue) and some selective competitors that show higher powers (TRP, GET, HDANOVA, marked in green); we exclude QuadMul since it shows almost zero power.

The numerical performance of our proposed depth statistic is remarkable, especially when it is based on the KD (13). It shows highest or comparable power over all scenarios. In particular, when shape alternatives are considered, the KD statistic is substantially powerful compared to the others. Among the depth statistics, following the KD, the RHD and IFD statistics stand in second place and generally perform comparably with the green statistics. The RHD mostly outperforms the IFD, except for the wiggle alternative scenarios. This could be anticipated as the RHD shows less sensitivity to functions of high frequency like

³<https://github.com/lidom/ffscb>

⁴<https://github.com/linulysses/hdanova>

Table 2: Empirical sizes of two-sample functional mean tests, when $n = 50$ and the FPC scores are of NN-type. Sizes within $[0.3, 0.7]$ are indicated in *italic*.

Eigenfunctions	Equal		Unequal	
Eigenvalues	Equal	Unequal	Equal	Unequal
ITD	<i>0.044</i>	<i>0.052</i>	<i>0.038</i>	<i>0.056</i>
IFD	<i>0.056</i>	<i>0.055</i>	<i>0.064</i>	0.082
RHD	<i>0.060</i>	<i>0.054</i>	0.074	<i>0.036</i>
KD	<i>0.069</i>	<i>0.067</i>	<i>0.064</i>	<i>0.056</i>
QuadInv	0.023	0.017	0.025	0.020
QuadMul	0.023	0.026	0.013	<i>0.033</i>
L2	<i>0.043</i>	<i>0.049</i>	<i>0.033</i>	<i>0.056</i>
sup	<i>0.035</i>	<i>0.038</i>	<i>0.036</i>	<i>0.056</i>
Fint	0.024	0.022	0.017	0.024
Fmax	0.015	0.016	0.011	0.011
Fmaxb	<i>0.037</i>	<i>0.045</i>	<i>0.049</i>	<i>0.065</i>
TRP	0.017	0.024	0.025	0.029
FP	<i>0.049</i>	<i>0.052</i>	<i>0.039</i>	<i>0.062</i>
HotSq	<i>0.050</i>	0.651	0.127	0.715
GET	<i>0.043</i>	<i>0.056</i>	<i>0.052</i>	<i>0.056</i>
FFSCB.t	0.078	0.086	0.091	0.097
Bs	0.002	0.004	0.002	0.010
BEc	0.414	0.295	0.414	0.404
naive.t	0.021	0.020	0.028	0.029
HDANOVA0	<i>0.042</i>	<i>0.039</i>	<i>0.030</i>	0.028
HDANOVA	<i>0.053</i>	<i>0.043</i>	<i>0.047</i>	<i>0.051</i>

$\mu_{2,\text{Wig}}$. The ITD essentially works well only when differences appear in magnitude (i.e., under magnitude, jump, and peak alternatives). This can be interpreted analogously to what happened in functional outlier detection; since the ITD is known to be weak in detecting shape outliers, the corresponding depth statistic could exhibit worse performance in rejecting shape alternatives. We refer to [Yeon et al. \(2025\)](#) for discussion of how a functional depth benefits functional outlier detection.

The main competitors tend to behave similarly; all of them perform worse than the KD, RHD, and IFD statistics under most scenarios. The power of these blue statistics heavily relies on the equality of covariance operators and alternative scenarios. For instance, in general, Fint performs worst when eigenfunctions are equal, while the power of sup statistic is the lowest in the other cases with unequal eigenfunctions. QuadInv works reasonably under

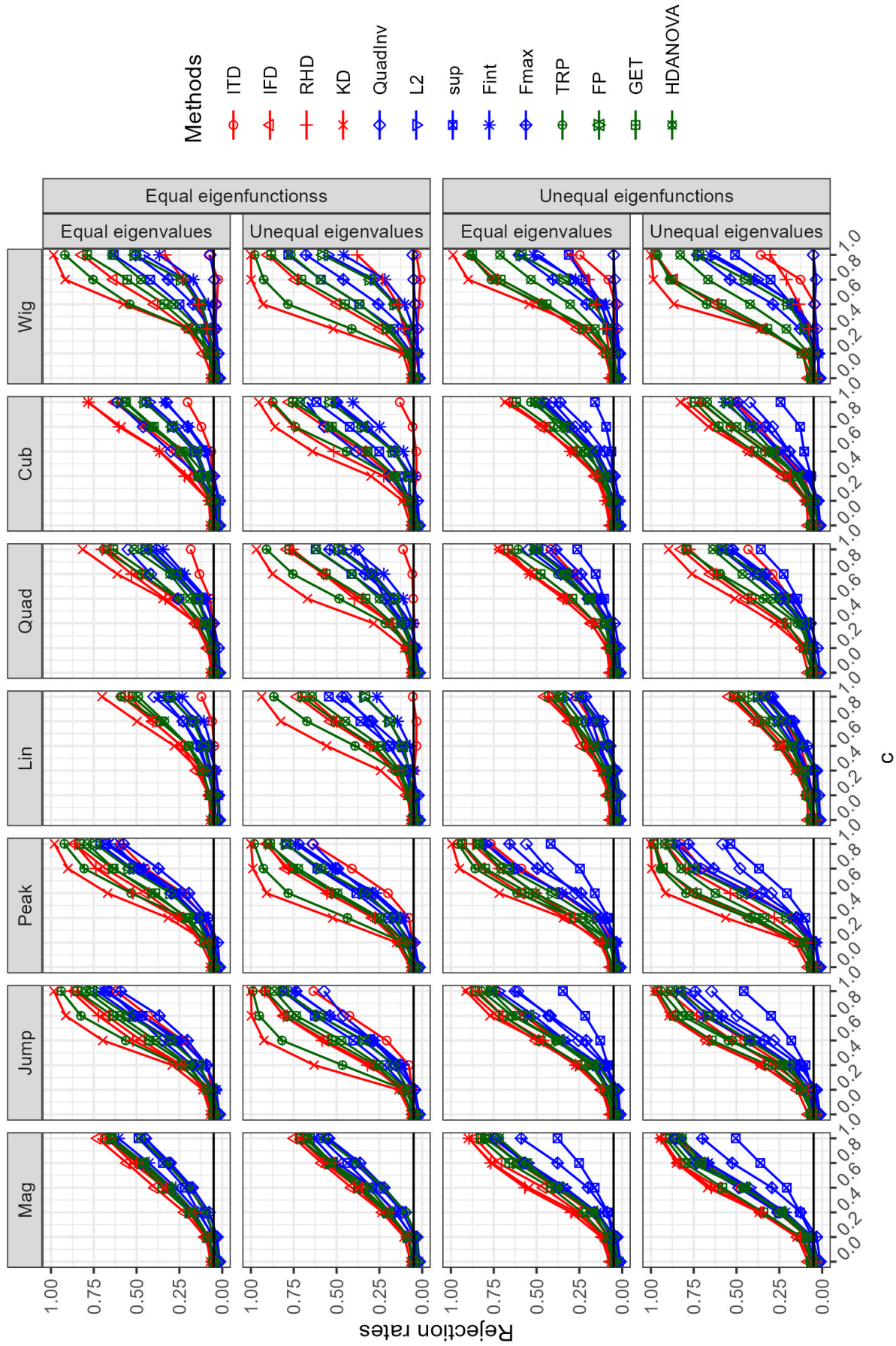


Figure 3: Empirical rejection rates of two-sample functional mean tests, when $n = 50$ and the FPC score are of NN-type.

magnitude, jump, and peak alternatives (even when covariance operators are different), but its performance becomes worse as the form of μ_2 is complicated; for $\mu_{2,\text{Wig}}$, it shows almost zero power. The other competing tests are reasonably powerful in general, although they perform worse than the KD statistic. In most cases, these green statistics work better than the blue statistics

The overall winner of this power analysis for two-sample problem is the proposed depth statistic based on the KD (13) with quantile level $u = 0.01$.

5.2 FoFR mean response inference

We continue our numerical analysis but under the FoFR setting in Section 3.2. Similarly to (15), the regressors $\{X_i\}_{i=1}^n$ and $\{\varepsilon_i\}_{i=1}^n$ are generated based on the KL expansion as $X_i = \sum_{j=1}^{J_{\text{true}}} \gamma_j^{1/2} \xi_{ij} \phi_j$ and $\varepsilon_i = \sum_{j=1}^{J_{\text{true}}} \delta_j^{1/2} \zeta_{ij} \psi_j$, respectively. The eigenvalues are determined through their gaps $\gamma_j - \gamma_{j+1} = 2j^{-a_X}$ and $\delta_j - \delta_{j+1} = 2j^{-a_\varepsilon}$ with $\gamma_1 = 2 \sum_{j=1}^{\infty} j^{-a_X}$ and $\delta_1 = 2 \sum_{j=1}^{\infty} j^{-a_\varepsilon}$ for some $a_X \in \{2.5, 3.5\}$ and $a_\varepsilon \in \{2.5, 3.5\}$, while the eigenfunctions are given as $\phi_j = \phi_{\text{mono},j}$ and $\psi_j = \phi_{\text{cheb},j}$. We set $\xi_{ij} \stackrel{d}{=} \xi_j$ and $\zeta_{ij} \stackrel{d}{=} \xi_j$, where only NN- and NE-type FPC scores are considered. The responses $\{Y_i\}_{i=1}^n$ are then computed based on the FoFR model (6) with zero intercept $\alpha = 0$ and slope operator \mathbf{B} described below. The sample sizes under consideration are $n \in \{50, 200, 1000\}$

To construct the slope operator \mathbf{B} , we first consider independent binary random variables $\{W_{\text{slope},j}\}$ such that $\mathbf{P}(W_{\text{slope},j} = 1) = 1/2 = \mathbf{P}(W_{\text{slope},j} = -1)$. With decay rate $b \in \{1.5, 2.5\}$ and $J_0 = 5$, the true slope operator $\mathbf{B} = \mathbf{B}_c$ is given by

$$\mathbf{B} \equiv (1 - c) \sum_{j=J_0+1}^{J_0} (2j^{-b}) W_{\text{slope},j} \phi_{\text{mono},j}^{\otimes 2} + c \sum_{j=1}^{2J_0} (2j^{-b}) W_{\text{slope},j} \phi_{\text{tri},j}^{\otimes 2}$$

for $c \in \{0, 0.2, 0.4, 0.6, 0.8, 1\}$. The new regressor is generated also based on a KL expansion as $X_0 \equiv \sum_{j=1}^{J_{\text{true}}} \gamma_{0j}^{1/2} \xi_{0j} \phi_{\text{mono},j}$ independently of $\{(Y_i, X_i)\}_{i=1}^n$, where $\gamma_{0j} = \gamma_j \mathbb{I}(j \leq J_0)$ and $\xi_{0j} \stackrel{d}{=} \xi_j$. We note that, when $c = 0$, it holds that $\mathbf{B}X_0 = 0 = \mathbf{B}\mathbf{E}[X_1]$, and hence it renders the null hypothesis $H_0 : \mu(X_0) = \mathbf{E}[Y]$.

For the residual bootstrap in (3.2), three truncation levels $J, J_{\text{res}}, J_{\text{cen}}$ are involved. Following the previous studies (Yeon, 2026+, Yeon et al., 2023), we choose J_{res} as the one minimizing prediction error estimated by the 5-fold cross-validation, and set $J_{\text{cen}} = J_{\text{res}}$. We then select J as the minimum of the truncation levels bigger than J_{cen} whose FVE exceed the threshold 0.85. This procedure is described in Section B.5 of the supplement.

For depth statistics, we only consider the RHD and the KD, as the frameworks for them and the FoFR residual bootstrap are commonly based on a Hilbert space. Since there are not many competing methods in this problem, we compare the RHD and KD statistics with L2 and supremum norms used by Yeon (2026+) and Dette and Tang (2024), respectively.

Since all tests achieve the nominal level well, we only provide their power curves.

Figure 4 shows empirical power of the tests under consideration, when $n = 50$, $a_X = a_\varepsilon = 2.5$, $b = 1.5$, and the FPC score are of NN-type. As in the two-sample problem, the depth statistics perform best. Notably, the RHD here performs slightly better than the KD. Another observations is that these depth statistics along with L2 statistic significantly outperforms the supremum statistic, where the latter can provide a simultaneous confidence band for \mathbf{B} . This may indicate that, like confidence bands for two-sample problem are not powerful, the ones for FoFR may not be effective for hypothesis testing.

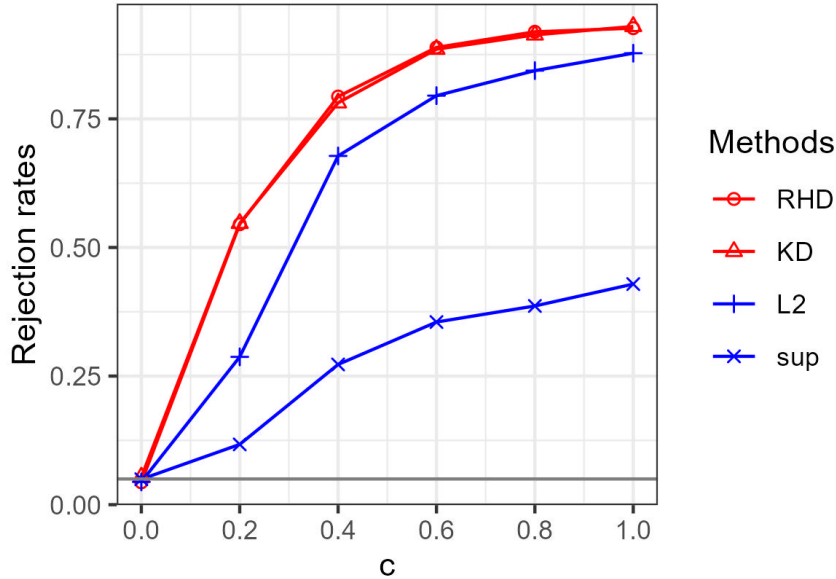


Figure 4: Empirical rejection rates for testing $H_0 : \mu(X_0) = \mathbf{E}[Y]$ in FoFR models, when $n = 50$, $a_X = a_\varepsilon = 2.5$, $b = 1.5$, and the FPC score are of NN-type.

5.3 Summary and guideline

In this section, upon summarizing our discoveries, we provide a concise guideline for using depth statistics based on our comprehensive numerical studies.

- (i) The KD statistics with $u = 0.01$ works best among all tests and in all scenarios for both two-sample problem and FoFR.
- (ii) The RHD statistic also works well in general and particularly for FoFR, but it may be weak in detecting extremely wiggle alternatives. The IFD statistic work well in general as well. Both RHD and IFD are comparable with other resampling-based methods (TRP, FP, HotSq, GET, HDANOVA0, HDANOVA).
- (iii) The classical summary statistics (QuadInv, QuadMul, L2, sup, Fint, Fmax) are less effective to detect complex forms of alternatives.

- (iv) Using confidence bands (e.g., FFSCB.t, BS, BEc, naive.t) may not be effective for hypothesis testing.

Based on these summarized observations, we recommend the depth statistic based on the KD with quantile level $u = 0.01$.

6 Data examples

6.1 Two-sample tests with Canadian weather data

We analyze the Canadian weather datasets. These are available from the Environment and Climate Change Canada website, and extracted using `weathercan` R package (LaZerte and Albers, 2018). We collect daily mean temperatures for years from 1962 to 2011, from stations 889, 2205, 5097, 5415, 6358 located in cities, Vancouver, Calgary, Toronto, Montreal, Halifax, respectively. Motivated by the abrupt increase in global average temperature around 1981 (cf. NOAA, 2024), for each city, we form two groups as the temperature curves of the first twenty years (1962-1981) and the later thirty years (1982-2011), yielding $\{X_{1i}\}_{i=1}^{n_1}$ and $\{X_{2i}\}_{i=1}^{n_2}$ with $n_1 = 20$ and $n_2 = 30$, respectively. We are interested in whether the mean temperature curves differ between these two groups.

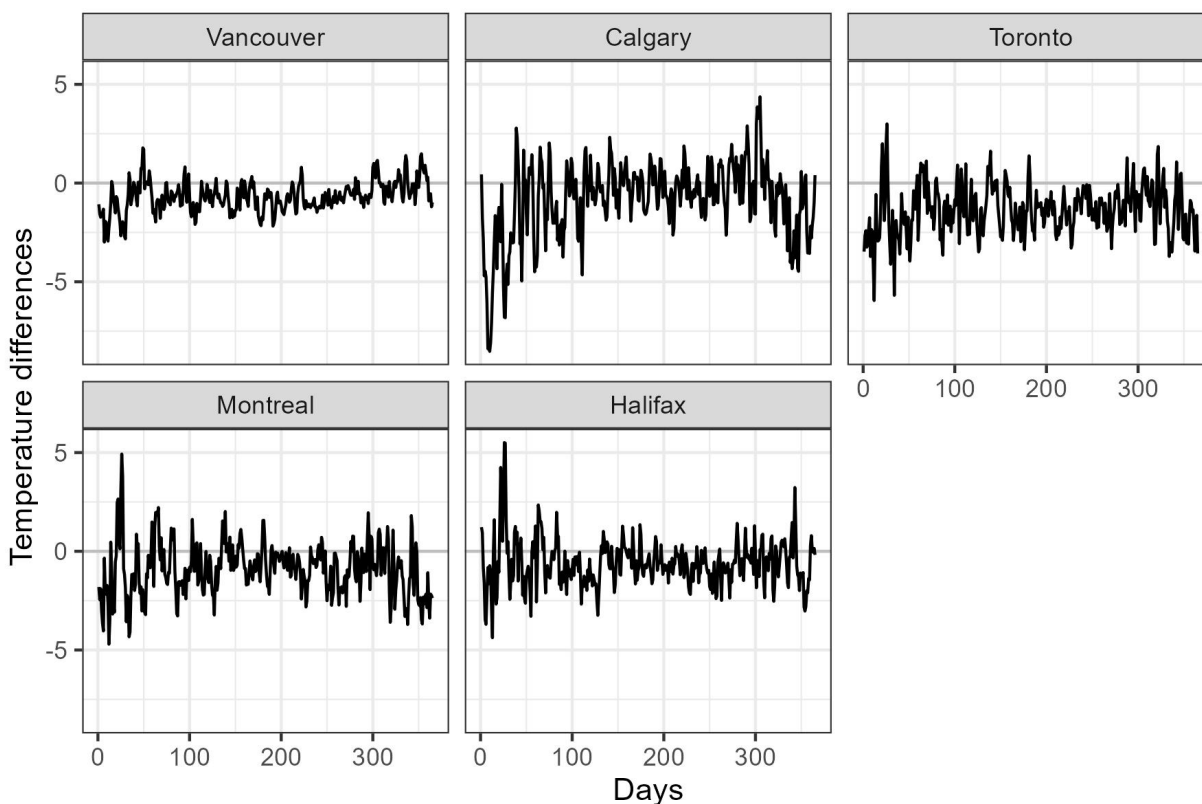


Figure 5: The differences between the temperature curves averaged over two groups of years 1962–1981 and 1982–2011. The horizontal line at zero is colored in gray.

The differences $\bar{X}_1 - \bar{X}_2$ in mean curves for each city are represented in [Figure 5](#). These curves show clear different from zero particularly in shape. We conduct the bootstrap two-sample functional mean tests with statistics as considered in [Section 5.1](#). In addition to the depth statistics, only our main competitors QuadInv, QuadMul, L2, sup, Fint, and Fmax are considered in this data analysis, as the sampling distributions of these statistics are approximated by the same resampling approach. We select the tuning parameter as implemented in [Section 5.1](#), when needed. The KD statistic produces a consistent result, which all explain significant differences in mean, while the other depth statistics sometimes provide weaker evidence depending on cities. Among the main competing tests, the L^2 statistic the most consistently rejects the null hypothesis, while the other tests sometimes exhibit very high p-values.

Table 3: The p-values from the bootstrap two-sample functional mean tests. We provide the results from the proposed depth statistics and our main competitors considered in [Section 5.1](#). Significant p-values no bigger than the level 0.05 are indicated in *italic*.

	ITD	IFD	RHD	KD	QuadInv	QuadMul	L2	sup	Fint	Fmax
Vancouver	<i>0.003</i>	<i>0.000</i>	<i>0.000</i>	<i>0.004</i>	<i>0.028</i>	0.143	<i>0.007</i>	0.238	<i>0.002</i>	<i>0.047</i>
Calgary	0.216	<i>0.000</i>	<i>0.033</i>	<i>0.050</i>	0.269	0.304	0.063	0.076	0.244	0.305
Toronto	<i>0.000</i>	<i>0.000</i>	<i>0.000</i>	<i>0.001</i>	<i>0.004</i>	0.080	<i>0.001</i>	<i>0.040</i>	<i>0.001</i>	0.185
Montreal	<i>0.013</i>	0.273	0.778	<i>0.028</i>	0.168	0.583	<i>0.039</i>	0.395	0.084	0.512
Halifax	<i>0.034</i>	<i>0.000</i>	0.937	<i>0.048</i>	0.558	0.913	0.060	0.059	0.075	0.291

6.2 Regression analysis of electricity prices on wind power in-feed

We illustrate the proposed depth statistic in FoFR framework in this section. We are interested in the relationship between electricity prices Y_i and the wind power in-feed (kWh) X_i in Germany. Both are treated as functions of time within a day, and the time was scaled into the unit interval $[0,1]$ before the analysis. This dataset was analyzed by [Liebl \(2013\)](#), where the original dataset can be found. We use the version with sample size $n = 591$, preprocessed by [Chagny et al. \(2025\)](#) for prediction in FoFR models. The observed regressor and response curves are presented with gray color in [Figure 6](#) with 20 randomly selected curves in black.

For illustration of the proposed method, we consider artificial new regressors resembling cubic, sine, and peak curves, scaled by $X_{\max} \equiv \max_{1 \leq i \leq n} \max_{0 \leq t \leq 1} X_i(t)$:

$$\begin{aligned}
 X_{0,\text{cub}}(t) &= X_{\max} \{4(t - 1/2)^3 + 1/2\}, \\
 X_{0,\text{sin}}(t) &= X_{\max} \{\sin(2\pi t)/2 + 1/2\}, \\
 X_{0,\text{peak}}(t) &= X_{\max} \mathbb{I}(0.3 \leq t \leq 0.7).
 \end{aligned}$$

The corresponding unobserved response curves are then expected to differ from the global

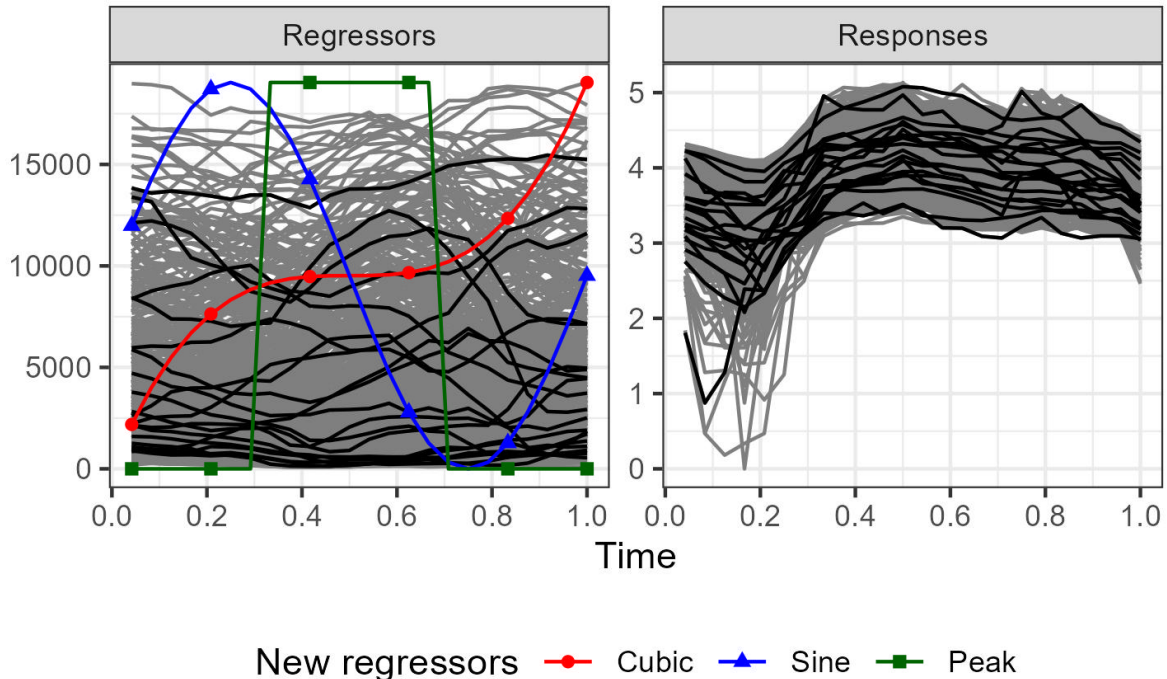


Figure 6: Regressor (wind power in-feed, kWh) and response (electricity prices) curves in gray. Twenty randomly selected curves are marked in black. Three artificial new regressors $\{X_{0,l} : l \in \{\text{cub}, \text{sin}, \text{peak}\}\}$ are indicated with red circles (cubic), blue triangles (sine), and green squares (peak).

mean response curve $\bar{Y} \equiv n^{-1} \sum_{i=1}^n Y_i$, due to their distinct patterns, thereby increasing the complexity of data analysis. These new regressor curves $\{X_{0,l} : l \in \{\text{cub}, \text{sin}, \text{peak}\}\}$ are shown in different colors and points in the left panel of Figure 6.

Table 4 shows the p-values from the bootstrap tests with the statistics considered in Section 5.2. The relevant tuning parameters are chosen as in Section 5.2. The depth statistics with RHD and KD consistently yield significant results, whereas the L^2 and supremum norm statistics provide weaker evidence. In particular, each of the latter two exhibits complementary strengths: the L^2 statistic is effective in detecting deviations of the new response at cubic and sine curves from the global mean response but less sensitive for the peak curve, while the supremum statistic shows the opposite pattern. In contrast, the proposed depth statistics produce robust and consistent results across all new regressors.

Data availability statement

The weather and wind power datasets analyzed in this paper can be obtained through the R package `weathercan` (LaZerte and Albers, 2018) and the work by Chagny et al. (2025), respectively.

Table 4: The p-values of the bootstrap tests with the statistics consider in [Section 5.2](#) for FoFR analysis of electricity prices on wind power in-feed. Significant p-values no bigger than the level 0.05 are indicated in *italic*.

	RHD	KD	L2	sup
Cubic	<i>0.031</i>	<i>0.037</i>	0.089	0.682
Sine	<i>0.000</i>	<i>0.000</i>	0.053	0.159
Peak	<i>0.000</i>	<i>0.000</i>	0.140	<i>0.011</i>

References

- Krishna B Athreya and Soumendra N Lahiri. *Measure Theory and Probability Theory*. Springer Science & Business Media, 2006.
- Alexander Aue, Holger Dette, and Gregory Rice. Two-sample tests for relevant differences in the eigenfunctions of covariance operators. *Statistica Sinica*, 33(1):353–379, 2023.
- Michal Benko, Wolfgang Härdle, and Alois Kneip. Common functional principal components. *Annals of Statistics*, 37(1):1–34, 2009.
- José R Berrendero, Beatriz Bueno-Larraz, and Antonio Cuevas. On Mahalanobis distance in functional settings. *Journal of Machine Learning Research*, 21(9):1–33, 2020.
- Patrick Billingsley. *Probability and Measure*. John Wiley & Sons, 1995.
- Patrick Billingsley. *Convergence of Probability Measures*. John Wiley & Sons, 1999.
- Graciela Boente, Matías Salibián Barrera, and David E Tyler. A characterization of elliptical distributions and some optimality properties of principal components for functional data. *Journal of Multivariate Analysis*, 131:254–264, 2014.
- Graciela Boente, Daniela Rodriguez, and Mariela Sued. Testing equality between several populations covariance operators. *Annals of the Institute of Statistical Mathematics*, 70(4):919–950, 2018.
- Denis Bosq. *Linear Processes in Function Spaces: Theory and Applications*, volume 149. Springer Science & Business Media, 2000.
- Florentina Bunea, Andrada E Ivanescu, and Marten H Wegkamp. Adaptive inference for the mean of a Gaussian process in functional data. *Journal of the Royal Statistical Society Series B: Statistical Methodology*, 73(4):531–558, 2011.
- Neal L Carothers. *A Short Course on Approximation Theory*. 1998.

- George Casella and Roger L. Berger. *Statistical Inference*. Cengage Learning, Pacific Grove, CA, 2 edition, 2002. ISBN 978-0534243128.
- Gaëlle Chagny, Anouar Meynaoui, and Angelina Roche. Adaptive nonparametric estimation in the functional linear model with functional output. *Electronic Journal of Statistics*, 19(1):2990–3039, 2025.
- Anirvan Chakraborty and Probal Chaudhuri. The spatial distribution in infinite dimensional spaces and related quantiles and depths. *Annals of Statistics*, 42(3), 2014.
- Chung Chang, Xuejing Lin, and R Todd Ogden. Simultaneous confidence bands for functional regression models. *Journal of Statistical Planning and Inference*, 188:67–81, 2017.
- Probal Chaudhuri. On a geometric notion of quantiles for multivariate data. *Journal of the American Statistical Association*, 91(434):862–872, 1996.
- Yan Chen, Hongmei Lin, Xueqin Wang, and Canhong Wen. A minimax two-sample test for functional data via Grothendieck’s divergence. *Journal of the American Statistical Association*, pages 1–25, 2025.
- Hyunphil Choi and Matthew Reimherr. A geometric approach to confidence regions and bands for functional parameters. *Journal of the Royal Statistical Society Series B: Statistical Methodology*, 80(1):239–260, 2018.
- Gerda Claeskens, Mia Hubert, Leen Slaets, and Kaveh Vakili. Multivariate functional half-space depth. *Journal of the American Statistical Association*, 109(505):411–423, 2014.
- Christophe Crambes and André Mas. Asymptotics of prediction in functional linear regression with functional outputs. *Bernoulli*, 19(5B):2627–2651, 2013.
- JA Cuesta-Albertos and Manuel Febrero-Bande. A simple multiway ANOVA for functional data. *Test*, 19(3):537–557, 2010.
- Antonio Cuevas, Manuel Febrero, and Ricardo Fraiman. An anova test for functional data. *Computational Statistics & Data Analysis*, 47(1):111–122, 2004.
- Antonio Cuevas, Manuel Febrero, and Ricardo Fraiman. On the use of the bootstrap for estimating functions with functional data. *Computational Statistics & Data Analysis*, 51(2):1063–1074, 2006.
- David A Degras. Simultaneous confidence bands for nonparametric regression with functional data. *Statistica Sinica*, pages 1735–1765, 2011.
- Holger Dette and Jiajun Tang. Statistical inference for function-on-function linear regression. *Bernoulli*, 30(1):304–331, 2024.

- Holger Dette, Kevin Kokot, and Alexander Aue. Functional data analysis in the Banach space of continuous functions. *Annals of Statistics*, 48(2):1168–1192, 2020.
- Subhajit Dutta, Anil K Ghosh, and Probal Chaudhuri. Some intriguing properties of Tukey’s half-space depth. *Bernoulli*, pages 1420–1434, 2011.
- Julian J Faraway. Regression analysis for a functional response. *Technometrics*, 39(3):254–261, 1997.
- Ricardo Fraiman and Graciela Muniz. Trimmed means for functional data. *Test*, 10:419–440, 2001.
- Stefan Fremdt, Josef G Steinebach, Lajos Horváth, and Piotr Kokoszka. Testing the equality of covariance operators in functional samples. *Scandinavian Journal of Statistics*, 40(1):138–152, 2013.
- Stefan Fremdt, Lajos Horváth, Piotr Kokoszka, and Josef G Steinebach. Functional data analysis with increasing number of projections. *Journal of Multivariate Analysis*, 124:313–332, 2014.
- Rahul Ghosal and Arnab Maity. A score based test for functional linear concurrent regression. *Econometrics and Statistics*, 21:114–130, 2022.
- Irène Gijbels and Stanislav Nagy. On a general definition of depth for functional data. *Statistical science*, 32(4):630–639, 2017.
- Felix Gnettner, Claudia Kirch, and Alicia Nieto-Reyes. Symmetrisation of a class of two-sample tests by mutually considering depth ranks including functional spaces. *Electronic Journal of Statistics*, 18(2):3021–3106, 2024.
- Tomasz Górecki and Lukasz Smaga. A comparison of tests for the one-way ANOVA problem for functional data. *Computational Statistics*, 30(4):987–1010, 2015.
- Tomasz Górecki and Lukasz Smaga. fdANOVA: an R software package for analysis of variance for univariate and multivariate functional data. *Computational Statistics*, 34(2):571–597, 2019.
- Jia Guo, Bu Zhou, and Jin-Ting Zhang. New tests for equality of several covariance functions for functional data. *Journal of the American Statistical Association*, 114(527):1251–1263, 2019.
- Peter Hall and Ingrid Van Keilegom. Two-sample tests in functional data analysis starting from discrete data. *Statistica Sinica*, pages 1511–1531, 2007.

- Zdeněk Hlávka, Daniel Hlubinka, and Kateřina Koňasová. Functional ANOVA based on empirical characteristic functionals. *Journal of Multivariate Analysis*, 189:104878, 2022.
- Lajos Horváth and Gregory Rice. Testing equality of means when the observations are from functional time series. *Journal of Time Series Analysis*, 36(1):84–108, 2015.
- Lajos Horváth, Piotr Kokoszka, and Ron Reeder. Estimation of the mean of functional time series and a two-sample problem. *Journal of the Royal Statistical Society Series B: Statistical Methodology*, 75(1):103–122, 2013.
- Tailen Hsing and Randall Eubank. *Theoretical Foundations of Functional Data Analysis, with an Introduction to Linear Operators*, volume 997. John Wiley & Sons, 2015.
- Mia Hubert, Peter Rousseeuw, and Pieter Segaert. Multivariate and functional classification using depth and distance. *Advances in Data Analysis and Classification*, 11(3):445–466, 2017.
- Jeong Min Jeon and Byeong U. Park. Additive regression with Hilbertian responses. *Ann. Statist.*, 48(5):2671–2697, 2020. ISSN 0090-5364,2168-8966.
- Piotr Kokoszka and Matthew Reimherr. *Introduction to Functional Data Analysis*. Chapman and Hall/CRC, 2017.
- Piotr Kokoszka, Inga Maslova, Jan Sojka, and Lie Zhu. Testing for lack of dependence in the functional linear model. *Canadian Journal of Statistics*, 36(2):207–222, 2008.
- David Kraus and Victor M Panaretos. Dispersion operators and resistant second-order functional data analysis. *Biometrika*, 99(4):813–832, 2012.
- Stefanie E LaZerte and Sam Albers. weathercan: Download and format weather data from environment and climate change canada. *The Journal of Open Source Software*, 3(22):571, 2018. URL <https://joss.theoj.org/papers/10.21105/joss.00571>.
- Dominik Liebl. Modeling and forecasting electricity spot prices: A functional data perspective. *Annals of Applied Statistics*, pages 1562–1592, 2013.
- Dominik Liebl and Matthew Reimherr. Fast and fair simultaneous confidence bands for functional parameters. *Journal of the Royal Statistical Society Series B: Statistical Methodology*, 85(3):842–868, 2023.
- Zhenhua Lin, Miles E Lopes, and Hans-Georg Müller. High-dimensional MANOVA via bootstrapping and its application to functional and sparse count data. *Journal of the American Statistical Association*, 118(541):177–191, 2023.

- Regina Y Liu. On a notion of data depth based on random simplices. *Annals of Statistics*, pages 405–414, 1990.
- Regina Y Liu and Kesar Singh. Notions of limiting p values based on data depth and bootstrap. *Journal of the American Statistical Association*, 92(437):266–277, 1997.
- Sara López-Pintado and Juan Romo. On the concept of depth for functional data. *Journal of the American statistical Association*, 104(486):718–734, 2009.
- Sara López-Pintado and Juan Romo. A half-region depth for functional data. *Computational Statistics & Data Analysis*, 55(4):1679–1695, 2011.
- Valentina Masarotto, Victor M Panaretos, and Yoav Zemel. Transportation-based functional ANOVA and PCA for covariance operators. *Electronic Journal of Statistics*, 18(1):1887–1916, 2024.
- Erik Mendroš and Stanislav Nagy. The spherical depth for functional data. In *International Workshop on Functional and Operatorial Statistics*, pages 401–408. Springer, 2025.
- Karl Mosler. *Multivariate Dispersion, Central Regions and Depth: The Lift Zonoid Approach*, volume 165 of *Lecture Notes in Statistics*. Springer-Verlag, Berlin, 2002. ISBN 0-387-95412-0.
- Karl Mosler. Depth statistics. *Robustness and Complex Data Structures: Festschrift in Honour of Ursula Gather*, pages 17–34, 2013.
- Tomáš Mrkvička, Mari Myllymäki, Milan Jílek, and Ute Hahn. A one-way ANOVA test for functional data with graphical interpretation. *Kybernetika*, 56(3):432–458, 2020.
- Mari Myllymäki and Tomáš Mrkvička. GET: Global envelopes in R. *Journal of Statistical Software*, 111(3):1–40, 2024. doi: 10.18637/jss.v111.i03.
- Stanislav Nagy, Irene Gijbels, and Daniel Hlubinka. Depth-based recognition of shape outlying functions. *Journal of Computational and Graphical Statistics*, 26(4):883–893, 2017.
- Naveen N Narisetty and Vijayan N Nair. Extremal depth for functional data and applications. *Journal of the American Statistical Association*, 111(516):1705–1714, 2016.
- NOAA. National Centers for Environmental Information, Climate at a Glance: Global Time Series. 2024. Published November 2024, retrieved on December 2, 2024 from <https://www.ncei.noaa.gov/access/monitoring/climate-at-a-glance/global/time-series>.
- Victor M Panaretos, David Kraus, and John H Maddocks. Second-order comparison of Gaussian random functions and the geometry of DNA minicircles. *Journal of the American Statistical Association*, 105(490):670–682, 2010.

- Efstathios Paparoditis and Theofanis Sapatinas. Bootstrap-based testing of equality of mean functions or equality of covariance operators for functional data. *Biometrika*, 103(3):727–733, 2016.
- Davide Pigoli, John AD Aston, Ian L Dryden, and Piercesare Secchi. Distances and inference for covariance operators. *Biometrika*, 101(2):409–422, 2014.
- Alessia Pini, Aymeric Stamm, and Simone Vantini. Hotelling’s T2 in separable Hilbert spaces. *Journal of Multivariate Analysis*, 167:284–305, 2018.
- Oleksii Pokotylo, Pavlo Mozharovskyi, and Rainer Dyckerhoff. Depth and depth-based classification with R package ddalpha. *Journal of Statistical Software*, 91(5):1–46, 2019. doi: 10.18637/jss.v091.i05.
- Zhuo Qu, Wenlin Dai, and Marc G Genton. Global depths for irregularly observed multivariate functional data. *arXiv preprint arXiv:2211.15125*, 2022.
- Kelly Ramsay and Shoja’eddin Chenouri. Robust nonparametric hypothesis tests for differences in the covariance structure of functional data. *Canadian Journal of Statistics*, 52(1):43–78, 2024.
- Hassan Sharghi Ghale-Joogh and S Mohammad E Hosseini-Nasab. A two-sample test for mean functions with increasing number of projections. *Statistics*, 52(4):852–873, 2018.
- Qing Shen and Julian Faraway. An F test for linear models with functional responses. *Statistica Sinica*, pages 1239–1257, 2004.
- Carl-Johann Simon-Gabriel, Alessandro Barp, Bernhard Schölkopf, and Lester Mackey. Metrizing weak convergence with maximum mean discrepancies. *Journal of Machine Learning Research*, 24(184):1–20, 2023.
- John W Tukey. Mathematics and the picturing of data. In *Proceedings of the International Congress of Mathematicians (Vancouver, B. C., 1974)*, volume 2, pages 523–531. Canadian Mathematical Congress, Montreal, Quebec, 1975.
- Honglang Wang, Ping-Shou Zhong, Yuehua Cui, and Yehua Li. Unified empirical likelihood ratio tests for functional concurrent linear models and the phase transition from sparse to dense functional data. *Journal of the Royal Statistical Society Series B: Statistical Methodology*, 80(2):343–364, 2018.
- George Wynne and Andrew B Duncan. A kernel two-sample test for functional data. *Journal of Machine Learning Research*, 23(73):1–51, 2022.

- George Wynne and Stanislav Nagy. Statistical depth meets machine learning: Kernel mean embeddings and depth in functional data analysis. *International Statistical Review*, 2025.
- Arthur B Yeh and Kesar Singh. Balanced confidence regions based on Tukey’s depth and the bootstrap. *Journal of the Royal Statistical Society Series B: Statistical Methodology*, 59(3):639–652, 1997.
- Hyemin Yeon. Inference for function-on-function regression: central limit theorem and residual bootstrap. *Statistics and Its Interface, To appear*, 2026+.
- Hyemin Yeon and Piotr Kokoszka. Bootstrap two-sample tests for functional regression. *Submitted*, 2026+.
- Hyemin Yeon, Xiongtao Dai, and Daniel J. Nordman. Bootstrap inference in functional linear regression models with scalar response. *Bernoulli*, 29(4):2599 – 2626, 2023.
- Hyemin Yeon, Xiongtao Dai, and Daniel J. Nordman. Bootstrap inference in functional linear regression models with scalar response under heteroscedasticity. *Electronic Journal of Statistics*, 18(2):3590 – 3627, 2024.
- Hyemin Yeon, Xiongtao Dai, and Sara Lopez-Pintado. Regularized halfspace depth for functional data. *Journal of the Royal Statistical Society Series B: Statistical Methodology*, 2025.
- Jin-Ting Zhang. Statistical inferences for linear models with functional responses. *Statistica Sinica*, pages 1431–1451, 2011.
- Jin-Ting Zhang and Jianwei Chen. Statistical inferences for functional data. *Annals of Statistics*, pages 1052–1079, 2007.
- Jin-Ting Zhang and Xuehua Liang. One-way ANOVA for functional data via globalizing the pointwise F-test. *Scandinavian Journal of Statistics*, 41(1):51–71, 2014.
- Jin-Ting Zhang, Ming-Yen Cheng, Hau-Tieng Wu, and Bu Zhou. A new test for functional one-way ANOVA with applications to ischemic heart screening. *Computational Statistics & Data Analysis*, 132:3–17, 2019.
- Xianyang Zhang and Xiaofeng Shao. Two sample inference for the second-order property of temporally dependent functional data. *Bernoulli*, 21(2):909–929, 2015.
- Yijun Zuo. Projection-based depth functions and associated medians. *Ann. Statist.*, 31(5): 1460–1490, 2003. ISSN 0090-5364.

Supplementary Material

Hyemin Yeon[†]

Department of Mathematical Sciences, Kent State University

This is a supplementary document of the manuscript titled “Effective and flexible depth-based inference for functional parameters”. This supplement includes technical and numerical details in Sections A–B, respectively.

A Theoretical details

A.1 Proof of the main results

Proof of Theorem 1. Write $A_n \equiv D(T_n; P_n) - D(T_n; P)$ so that

$$|A_n| \leq \sup_{x \in \mathbb{H}} |D(x; P_n) - D(x; P)| \rightarrow 0.$$

Note that this convergence holds due to Condition (C1) and (C4). Then, by Condition (C1) and (C3), we further observe

$$D(T_n; P_n) = D(T_n; P) + A_n \xrightarrow{d} D(T; P).$$

By the Polya’s theorem (Athreya and Lahiri, 2006, Theorem 9.1.4) and Condition (C5), we have

$$\sup_{u \in \mathbb{R}} |\mathbb{P}(D(T_n; P_n) \leq u) - \mathbb{P}(D(T; P) \leq u)| \rightarrow 0.$$

Similarly, we consider $A_n^* \equiv D(T_n^*; \widehat{P}_n) - D(T_n^*; P)$ so that

$$|A_n^*| \leq \sup_{x \in \mathbb{H}} |D(x; \widehat{P}_n) - D(x; P)| \xrightarrow{\mathbb{P}} 0,$$

due to Conditions (C1), (C2), and (C4). This is derived by using a subsequence argument (e.g., Billingsley, 1995, Theorem 20.5). Then, using Conditions (C3) and (C5), and the Polya’s theorem (Athreya and Lahiri, 2006, Theorem 9.1.4), we have (possibly following a subsequence) that

$$\sup_{u \in \mathbb{R}} |\mathbb{P}^*(D(T_n^*; \widehat{P}_n) \leq u) - \mathbb{P}(D(T; P) \leq u)| \xrightarrow{\mathbb{P}} 0.$$

This concludes the desired result. ■

Proof of Theorem 2. First, by Theorem 1, we have

$$|\widehat{F}_n(D(T_n; \widehat{P}_n)) - F(D(T_n; \widehat{P}_n))| \leq \sup_{u \in \mathbb{R}} |\widehat{F}_n(u) - F(u)| \xrightarrow{\mathbb{P}} 0$$

[†]hyeon1@kent.edu

Using Conditions (C1), (C3), and (C4), we also observe that

$$\begin{aligned} |D(T_n; \widehat{P}_n) - D(T_n; P)| &\leq \sup_{x \in \mathbb{H}} |D(x; P_n) - D(x; P)| \rightarrow 0, \\ |D(T_n; P) - D(T; P)| &\leq \sup_{P \in \mathcal{P}(\mathbb{H})} |D(T_n; P) - D(T; P)| \xrightarrow{\mathbb{P}} 0, \end{aligned}$$

implying $D(T_n; \widehat{P}_n) \xrightarrow{\mathbb{P}} D(T; P)$. Here, deriving the second result may require a subsequence argument (e.g., Billingsley, 1995, Theorem 20.5). The probability integral transform along with Slutsky's theorem (cf. Billingsley, 1999, Theorem 3.1) concludes

$$\widehat{\pi}_n = \widehat{F}_n(D(T_n; \widehat{P}_n)) - F(D(T_n; \widehat{P}_n)) + F(D(T_n; \widehat{P}_n)) \xrightarrow{d} F(D(T; P)) \sim \text{Unif}(0, 1).$$

■

A.2 Proof for the two-sample functional mean tests

Proof of Theorem 3. By a central limit theorem in a general Hilbert space (e.g., Hsing and Eubank, 2015, Theorem 7.7.6), we have

$$\begin{aligned} \sqrt{\frac{n_1 n_2}{n_1 + n_2}} (\bar{X}_1 - \mu_1) &\xrightarrow{d} \mathbf{G}(0, (1 - \zeta)\Gamma_1), \\ \sqrt{\frac{n_1 n_2}{n_1 + n_2}} (\bar{X}_2 - \mu_2) &\xrightarrow{d} \mathbf{G}(0, \zeta\Gamma_2), \end{aligned}$$

implying

$$T_{\text{two}, \mathbf{n}} = \sqrt{\frac{n_1 n_2}{n_1 + n_2}} (\bar{X}_1 - \bar{X}_2) \xrightarrow{d} \mathbf{G}(0, (1 - \zeta)\Gamma_1 + \zeta\Gamma_2).$$

Here, $\mathbf{G}(0, (1 - \zeta)\Gamma_1 + \zeta\Gamma_2)$ stands for the Gaussian distribution on \mathbb{H} with mean zero and covariance $(1 - \zeta)\Gamma_1 + \zeta\Gamma_2$. This derives the first result.

For the second part, let $E_k \equiv (\widehat{\Gamma}_k \rightarrow \Gamma_k)$ for $k = 1, 2$ and $E \equiv E_1 \cap E_2$ so that $\mathbf{P}(E) = 1$ by the law of large numbers (Hsing and Eubank, 2015, Theorem 7.7.5). Then, on E , we have the following observations. Write $\bar{\varepsilon}_k^* \equiv n_k^{-1} \sum_{i=1}^{n_k} \varepsilon_{ki}^*$. Using $\mathbf{E}^*[\varepsilon_{ki}^*] = 0$, $\mathbf{var}^*[\varepsilon_{ki}^*] = \mathbf{E}^*[(\varepsilon_{ki}^*)^{\otimes 2}] = \widehat{\Gamma}_k$, and the independence between $\{\varepsilon_{ki}^*\}_{i=1}^{n_k}$, we can see that $\sqrt{n_k} \bar{\varepsilon}_k^*$ is tight with respect to \mathbf{P}^* , because

$$\mathbf{E}^*[\|\sqrt{n_k} \bar{\varepsilon}_k^*\|^2] \leq \mathbf{E}^*[\|\varepsilon_k^*\|^2] = \text{tr}(\mathbf{var}^*[\varepsilon_k^*]) = \text{tr}(\widehat{\Gamma}_k) \rightarrow \text{tr}(\Gamma_k),$$

implying

$$\limsup_{n \rightarrow \infty} \mathbf{P}(\|\sqrt{n_k} \bar{\varepsilon}_k^*\| > M) \leq M^{-2} \text{tr}(\Gamma_k) \rightarrow 0, \quad \text{as } M \rightarrow \infty.$$

Also, let $v \in \mathbb{H}$ so that $\mathbf{E}^*[\langle \varepsilon_{ki}^*, v \rangle] = 0$ and $\mathbf{var}^*[\langle \varepsilon_{ki}^*, v \rangle] = \langle \widehat{\Gamma}_k v, v \rangle \rightarrow \langle \Gamma_k v, v \rangle$. Then, following

\mathbf{P}^* , we have

$$\langle \Gamma_k v, v \rangle^{-1/2} \langle \sqrt{n_k} \bar{\varepsilon}_k^*, v \rangle = \left(\frac{\langle \hat{\Gamma}_k v, v \rangle}{\langle \Gamma_k v, v \rangle} \right)^{1/2} \sqrt{n_k n_k^{-1}} \sum_{i=1}^{n_k} \langle \hat{\Gamma}_k v, v \rangle^{-1/2} \langle \varepsilon_{ki}^*, v \rangle \xrightarrow{d} \mathbf{N}(0, 1),$$

i.e., $\langle \sqrt{n_k} \bar{\varepsilon}_k^*, v \rangle \xrightarrow{d} \mathbf{N}(0, \langle \Gamma_k v, v \rangle)$. In brief, on E , (Bosq, 2000, Theorem 2.3) implies that $\sqrt{n_k} \bar{\varepsilon}_k^*$ converges in distribution to $\mathbf{G}(0, \Gamma_k)$ for each $k = 1, 2$, implying that

$$T_{\text{two}, \mathbf{n}}^* = \sqrt{\frac{n_1 n_2}{n_1 + n_2}} (\bar{\varepsilon}_1^* - \bar{\varepsilon}_2^*) \xrightarrow{d} \mathbf{G}(0, (1 - \zeta)\Gamma_1 + \zeta\Gamma_2).$$

Since $\mathbf{P}(E) = 1$, this concludes part (b). ■

A.3 Continuity of the kernel depth

Write $\mathcal{P}(\mathbb{H})$ for the set of all probability measures on \mathbb{H} . We start with a series of definitions related to the kernel theory. We refer to Wynne and Nagy (2025) for a recent theory for kernel-based methods in Statistics and Machine Learning.

Definition 1. We call a function $\kappa : \mathbb{H} \times \mathbb{H} \rightarrow \mathbb{R}$ a *kernel* on \mathbb{H} if

- (a) κ is symmetric as $\kappa(x, y) = \kappa(y, x)$ for all $x \in \mathbb{H}$ and $y \in \mathbb{H}$, and
- (b) κ is positive definite, i.e., $\sum_{j=1}^p \sum_{j'=1}^p \kappa(x_j, x_{j'}) \geq 0$ for all $(x_1, \dots, x_p) \in \mathbb{H}^p$, $(a_1, \dots, a_p) \in \mathbb{R}^p$, and $p \in \mathbb{N}$.

Definition 2. For a kernel κ , a Hilbert space $\mathbb{G}(\kappa)$ of functions from \mathbb{H} to \mathbb{R} is called a *reproducing kernel Hilbert space (RKHS)* if

- (a) $\kappa(\cdot, x) \in \mathbb{G}(\kappa)$ for all $x \in \mathbb{H}$, and
- (b) (reproducing property) $\langle g, \kappa(\cdot, x) \rangle_\kappa = g(x)$ for all $g \in \mathbb{G}(\kappa)$ and $x \in \mathbb{H}$.

Definition 3. For a kernel κ , we define the *kernel mean embedding (KME)* $\mathcal{E}_\kappa : \mathcal{P}(\mathbb{H}) \rightarrow \mathbb{G}(\kappa)$ as $\mathcal{E}_\kappa(P) = \int \kappa(\cdot, x) dP(x)$ for $P \in \mathcal{P}(\mathbb{H})$, i.e.,

$$\{\mathcal{E}_\kappa(P)\}(x) = \int \kappa(x, y) dP(y), \quad x \in \mathbb{H}, \quad P \in \mathcal{P}(\mathbb{H}).$$

We observe that, for $g \in \mathbb{G}(\kappa)$ and $P \in \mathcal{P}(\mathbb{H})$,

$$\langle \mathcal{E}_\kappa P, g \rangle_\kappa = \int \langle \kappa(\cdot, x), g \rangle dP(x) = \int g(x) dP(x) = \int g dP,$$

and hence, $\langle \mathcal{E}_\kappa P, \kappa(\cdot, x) \rangle_\kappa = \{\mathcal{E}_\kappa(P)\}(x)$ for all $x \in \mathbb{H}$.

With a slight abuse of notation, we define an inner product between P and Q with respect to κ as $\langle P, Q \rangle_\kappa \equiv \langle \mathcal{E}_\kappa P, \mathcal{E}_\kappa Q \rangle_\kappa$ for $P \in \mathcal{P}(\mathbb{H})$ and $Q \in \mathcal{P}(\mathbb{H})$. When κ is Gaussian, i.e., $\kappa(x, y) = e^{-\|x-y\|^2/2}$, $x \in \mathbb{H}$, $y \in \mathbb{H}$, it indeed induces an inner product on $\mathcal{P}(\mathbb{H})$ as κ

is characteristic by [Wynne and Nagy \(2025, Theorem 11\)](#). Note that, for $P \in \mathcal{P}(\mathbb{H})$ and $Q \in \mathcal{P}(\mathbb{H})$,

$$\langle P, Q \rangle_\kappa = \langle \mathcal{E}_\kappa P, \mathcal{E}_\kappa Q \rangle_\kappa = \int \int \kappa(x, y) dP(x) dQ(y) = (P \otimes Q)(\kappa),$$

where $P \otimes Q$ represents the product measure of P and Q (cf. [Billingsley, 1999, Section 2](#)). In particular, the corresponding distance $\|P - Q\|_\kappa \equiv \langle P - Q, P - Q \rangle_\kappa^{1/2}$ between P and Q is called the *maximum mean discrepancy (MMD)* ([Wynne and Nagy, 2025, Definition 5](#)).

The following lemma states that the weak convergence of probability measures implies the convergence in MMD.

Lemma 1. *Let κ be a bounded and continuous kernel on \mathbb{H} . For a sequence $\{P_n\}$ in $\mathcal{P}(\mathbb{H})$ and $P \in \mathcal{P}(\mathbb{H})$, as $n \rightarrow \infty$, if P_n weakly converges to P , then $\|P_n - P\|_\kappa \rightarrow 0$.*

Proof. We follow the argument in the proof of [Simon-Gabriel et al. \(2023, Lemma 5\(iv\) \$\Rightarrow\$ \(i\)\)](#). Due to the weak convergence of $\{P_n\}$ to P , [Billingsley \(1999, Theorem 2.8\(ii\)\)](#) yields that $P_n \otimes P$, $P \otimes P_n$, and $P_n \otimes P_n$ all weakly converge to $P \otimes P$. Since κ is also bounded and continuous, we have

$$\begin{aligned} \|P_n - P\|_\kappa^2 &= \langle P_n, P_n \rangle_\kappa - \langle P_n, P \rangle_\kappa - \langle P, P_n \rangle_\kappa + \langle P, P \rangle_\kappa \\ &= (P_n \otimes P_n)(\kappa) - (P_n \otimes P)(\kappa) + (P \otimes P_n)(\kappa) + (P \otimes P)(\kappa) \rightarrow 0. \end{aligned}$$

■

Proof of Theorem 5. We define $\kappa : \mathbb{H} \times \mathbb{H} \rightarrow \mathbb{R}$ by $\kappa(x, y) \equiv K(\|x - y\|)$ for $x \in \mathbb{H}$ and $y \in \mathbb{H}$. Due to the equivalence between KME (induced by κ) and the KD (determined by K) in [Wynne and Nagy \(2025, Theorem 1\)](#), it suffice to show the convergence upon embedding the probability measures into $\mathbb{G}(\kappa)$.

The first part is derived as follows. Using the symmetry of the kernel κ and its reproducing property, we find that, for each $x \in \mathbb{H}$ and $y \in \mathbb{H}$,

$$\|\kappa(\cdot, x) - \kappa(\cdot, y)\|_\kappa^2 = \kappa(x, x) + \kappa(y, y) - 2\kappa(x, y).$$

This implies that $\|\kappa(\cdot, x_n) - \kappa(\cdot, x)\|_\kappa \rightarrow 0$ as $x_n \rightarrow x$ due to the continuity of κ . On the other hand, the boundedness of κ yields

$$\sup_{P \in \mathcal{P}(\mathbb{H})} \|\mathcal{E}_\kappa P\|_\kappa^2 = \sup_{P \in \mathcal{P}(\mathbb{H})} \int \int \kappa(x, y) dP(x) dP(y) \leq \sup_{x \in \mathbb{H}} \kappa(x, x) < \infty.$$

Combining these, we conclude that

$$\begin{aligned} \sup_{P \in \mathcal{P}(\mathbb{H})} |\mathcal{E}_\kappa P(x_n) - \mathcal{E}_\kappa P(x)| &= \sup_{P \in \mathcal{P}(\mathbb{H})} | \langle \mathcal{E}_\kappa P, \kappa(\cdot, x_n) \rangle_\kappa - \langle \mathcal{E}_\kappa P, \kappa(\cdot, x) \rangle_\kappa | \\ &\leq \|\kappa(\cdot, x_n) - \kappa(\cdot, x)\|_\kappa \sup_{P \in \mathcal{P}(\mathbb{H})} \|\mathcal{E}_\kappa P\|_\kappa \rightarrow 0. \end{aligned}$$

Next, we prove part (b). Following the proof of [Wynne and Nagy \(2025, Theorem 5\)](#),

since $\|\kappa(\cdot, x)\|_\kappa^2 = \kappa(x, x)$ for $x \in \mathbb{H}$, it holds as

$$\begin{aligned} \sup_{x \in \mathbb{H}} |\mathcal{E}_\kappa P_n(x) - \mathcal{E}_\kappa P(x)| &= \sup_{x \in \mathbb{H}} |\langle \mathcal{E}_\kappa P_n, \kappa(\cdot, x) \rangle_\kappa - \langle \mathcal{E}_\kappa P, \kappa(\cdot, x) \rangle_\kappa| \\ &\leq \sup_{x \in \mathbb{H}} \|\kappa(\cdot, x)\|_\kappa \|\mathcal{E}_\kappa P_n - \mathcal{E}_\kappa P\|_\kappa \\ &= \sup_{x \in \mathbb{H}} \sqrt{\kappa(x, x)} \|P_n - P\|_\kappa \rightarrow 0, \end{aligned}$$

where the last convergence follows by [Lemma 1](#). ■

A.4 Nondegeneracy of the modified RHD

We provide a nondegeneracy result for the modified RHD given in [Section 4.2](#) under a mild condition, which includes all elliptically-contoured functional data ([Boente et al., 2014](#)).

Theorem 6. *Let $Q \in \mathcal{P}(\mathbb{H})$ and we write*

$$\mathcal{V}_\lambda(Q) \equiv \{v \in \mathbb{H} : \|v\| = 1, \|\Gamma(Q)^{1/2}v\| \geq \lambda\}.$$

Suppose that

$$\sup_{v \in \mathcal{V}_\lambda(Q)} \mathbf{P} \left(\frac{\langle X - \mathbf{E}[X], v \rangle}{\|\Gamma(Q)^{1/2}v\|} \leq u \right) < 1. \quad (\text{A.16})$$

Then, $D_{\text{RHD}, \lambda}(x; Q) > 0$ for all $x \in \mathbb{H}$.

Proof. This holds because

$$\begin{aligned} D_\lambda(x; Q) &= \inf_{v \in \mathcal{V}_\lambda(Q)} \mathbf{P}(\langle X, v \rangle \geq \langle x, v \rangle) \\ &= 1 - \sup_{v \in \mathcal{V}_\lambda(Q)} \mathbf{P} \left(\frac{\langle X - \mathbf{E}[X], v \rangle}{\|\Gamma(Q)^{1/2}v\|} \leq \frac{\langle x - \mu, v \rangle}{\|\Gamma(Q)^{1/2}v\|} \right) > 0. \end{aligned}$$

■

A.5 Assumptions for FoFR residual bootstrap consistency

We provide the technical conditions that are sufficient for the residual bootstrap consistency for function-on-function regression in [Theorem 4](#); we refer to [Yeon \(2026+\)](#) for more details about its theoretical development and an example that satisfies all these conditions (Example 1 therein). We write $\Gamma \equiv \mathbf{E}[(X - \mathbf{E}[X])^{\otimes 2}]$ for the covariance operator of X with its spectral decomposition $\Gamma = \sum_{j=1}^{\infty} \gamma_j(\phi_j \otimes \phi_j)$, where (γ_j, ϕ_j) denotes its j -th eigenvalue-eigenfunction pair. [Theorem 4](#) holds under the following conditions:

(A0) $\ker \Gamma = \{0\}$;

(A1) the slope operator \mathbf{B} is a Hilbert–Schmidt operator on \mathbb{H} such that the sequence

$$\left\{ \sum_{j'=1}^{\infty} \langle \mathbf{B}\phi_j, \phi_{j'} \rangle^2 \right\}_{j=1}^{\infty}$$

is non-increasing;

(A2) $\sup_{j \in \mathbb{N}} \gamma_j^{-2} \mathbf{E}[\langle X_1 - \mathbf{E}[X_1], \phi_j \rangle^4] < \infty$;

(A3) the eigenvalues $\{\gamma_j\}_{j=1}^{\infty}$ satisfy $\gamma_j = \varphi(j)$ for sufficiently large j , where $\varphi : (0, \infty) \rightarrow (0, \infty)$ is a convex function;

(A4) $\sup_{j \in \mathbb{N}} \gamma_j j \log j < \infty$;

(A5) $J^{-1} + n^{-1/2} J^2 \log J + n^{-1} \sum_{j=1}^J \delta_j^{-2} \rightarrow 0$ as $n \rightarrow \infty$, where $\{\delta_j\}$ are eigengaps defined as $\delta_j \equiv \gamma_1 - \gamma_2$ if $j = 1$ and $\delta_j \equiv \min\{\gamma_j - \gamma_{j+1}, \gamma_{j-1} - \gamma_j\}$ if $j > 1$ otherwise;

(B) $\sup_{j \in \mathbb{N}} j^{-1} m(j, u) \|B\phi_j\|^2 < \infty$ for $u > 5$,

where

$$m(j, u) \equiv \max \left\{ j^u, \sum_{l=1}^j \delta_l^{-2} \right\}, \quad j \in \mathbb{N}, \quad u > 0; \quad (\text{A.17})$$

(S) $J\tau_J(X_0)^{-1} = O_{\mathbf{P}}(1)$, where $\tau_J(x) \equiv \sum_{j=1}^J \gamma_j^{-1} \langle x - \mathbf{E}[X_1], \phi_j \rangle^2$ for $x \in \mathbb{H}$;

(E) there exists a class $\{g_x\}_{x \in \mathbb{H}}$ of (non-random) functions on $[0, \infty)$ to $[0, \infty)$ with $\lim_{u \rightarrow \infty} g_x(u) = 0$ for each $x \in \mathbb{H}$ such that $\mathbf{E}[\langle \varepsilon, x \rangle^2 \mathbb{I}(|\langle \varepsilon, x \rangle| \geq u) | X] \leq g_x(u)$ almost surely for any $u \geq 0$ and $x \in \mathbb{H}$;

(R) $\lim_{n \rightarrow \infty} J/J_{\text{cen}} \geq 1$;

(O) the truncation levels J_{res} and J_{cen} satisfy Condition (A5) and Condition (S) holds for J_{cen} ; and

(T) $n^{-1/2} J^{5/2} (\log J)^J \rightarrow 0$ and $n = O(m(J, u))$ for $u > 5$.

B Some details in numerical studies

B.1 Implementation of the RHD

The sample counterpart of the RHD of $x \in \mathbb{H}$ in Equation (14) of Section 4.2 is given as

$$D_{\text{RHD}, \lambda}(x; \widehat{Q}_n) = \inf_{v \in \mathcal{V}_{\lambda}(\widehat{Q}_n)} n^{-1} \sum_{i=1}^n \mathbb{I}(\langle X_i - x, v \rangle \geq 0).$$

We adopt a random projection approach to approximate the sample RHD $D_{\text{RHD},\lambda}(x; \widehat{Q}_n)$. We first draw M random directions $\{\tilde{v}_m\}_{m=1}^M$ from $\mathcal{V}_\lambda(\widehat{Q}_n)$ and then compute the minimum instead of the infimum:

$$\tilde{D}_{\text{RHD},\lambda}(x; \widehat{Q}_n) \equiv \min_{1 \leq m \leq M} n^{-1} \sum_{i=1}^n \mathbb{I}(\langle X_i - x, v_m \rangle \geq 0).$$

To explain our tie-breaking approach, we first find a direction that shows the largest outlyingness. Namely, for each x , we may find $L = L(x)$ minimizers as

$$\{\tilde{w}_1(x), \dots, \tilde{w}_L(x)\} = \underset{\tilde{v} \in \{\tilde{v}_m\}_{m=1}^M}{\operatorname{argmin}} n^{-1} \sum_{i=1}^n \mathbb{I}(\langle X_i - x, v_m \rangle \geq 0).$$

and take average to obtain $\bar{w}(x) \equiv L^{-1} \sum_{l=1}^L \tilde{w}_l(x)$. We now consider the outlyingness $O_{\bar{w}(x)}(x; \widehat{Q}_n)$ of the projection of x onto $\bar{w}(x)$, where

$$O_v(x; P) \equiv \frac{|\langle x, v \rangle - \operatorname{med}[\langle X, v \rangle]|}{\operatorname{MAD}[\langle X, v \rangle]}$$

with median med and median absolute deviation MAD operators.

Suppose we have several x_1, \dots, x_Q that are tied in RHD rankings. Then, we break these ties using the outlyingness in the projection directions $\{\bar{w}(x_q)\}_{q=1}^Q$ that minimize the halfspace probabilities. That is, the rankings of $\{O_{\bar{w}(x_q)}(x_q; \widehat{Q}_n)\}_{q=1}^Q$ are assigned to the rankings of $\{x_q\}_{q=1}^Q$, where lower rankings mean higher outlyingness $O_v(x)$.

B.2 Orthogonal systems

We provide the detailed constructions of the orthonormal systems used for the numerical studies in [Section 5.1](#), which are also adopted by [Yeon and Kokoszka \(2026+\)](#). The trigonometric functions $\{\phi_{\text{tri},j}\}_{j=1}^{J_{\text{true}}}$ are defined as

$$\phi_{\text{tri},1}(t) = 1, \phi_{\text{tri},2m}(t) = \sqrt{2} \sin(2m\pi t), \phi_{\text{tri},2m+1}(t) = \sqrt{2} \cos(2m\pi t), m \in \mathbb{N}.$$

For the remaining three orthonormal systems, we use the following three sets $\{f_{q,j}\}_{j=1}^{J_{\text{true}}}$ for $q \in \{\text{mono}, \text{cheb}, \text{spl}\}$ of linearly independent functions.

Monomials:

$$f_{\text{mono},j}(t) = t^j, \quad t \in [0, 1], \quad j = 1, \dots, J_{\text{true}}.$$

Shifted Chebyshev polynomials: The (unshifted) Chebyshev polynomials $\{f_{\text{cheb},j}\}_{j=1}^{J_{\text{true}}}$ of the first kind are determined by the recurrence formula $f_{\text{cheb},\text{unshift},j}(s) = 2s f_{\text{cheb},\text{unshift},j-1}(s) + f_{\text{cheb},\text{unshift},j-2}(s)$ for $j \geq 2$ with $f_{\text{cheb},\text{unshift},1}(s) = s$ and $f_{\text{cheb},\text{unshift},0}(s) = 1$ where $s \in [-1, 1]$ ([Carothers, 1998](#), Chapter 3); these are implemented by `chebPoly` function in `pracma` R

package. We shift them to $[0, 1]$

$$f_{\text{cheb},j}(t) = f_{\text{cheb,unshift},j}(2t - 1), \quad t \in [0, 1], \quad j = 1, \dots, J_{\text{true}}.$$

B-spline basis functions of order 4: We use `create.bspline.basis` function in `fda` package to create well-known B-spline basis functions of order 4 (i.e., cubic splines) and denote them by $\{f_{\text{spl},j}\}_{j=1}^{J_{\text{true}}}$.

For each $q \in \{\text{mono, cheb, spl}\}$, we orthogonalize the set $\{f_{q,j}\}_{j=1}^{J_{\text{true}}}$ by using the Gram–Schmidt orthogonalization (Hsing and Eubank, 2015, Theorem 2.4.10), then normalize them to unit norm, and the resulting orthonormal system is denoted as $\{\phi_{q,j}\}_{j=1}^{J_{\text{true}}}$.

B.3 Construction of alternative mean functions

In this section, we provide the alternative mean functions considered for the numerical studies in Section 5.1, which are plotted in Figure 2.

- $\mu_{2,\text{Mag}}(t) = 1$
- $\mu_{2,\text{Jump}}(t) = -2\mathbb{I}(t \leq 0.2) + 1$
- $\mu_{2,\text{Peak}}(t) = -2\mathbb{I}(0.2 < t \leq 0.4) + 1$
- $\mu_{2,\text{Lin}}(t) = 2t - 1$
- $\mu_{2,\text{Quad}}(t) = 8(t - 1/2)^2 - 1$
- $\mu_{2,\text{Cub}}(t) = 12\sqrt{3}t(t - 1/2)(t - 1)$
- $\mu_{2,\text{Wig}}(t) = \sin(10\pi(t - 0.05))$

B.4 Implementation of the classical summary statistics for two-sample inference

In the two-sample framework in Section 3.1, let $\widehat{\Gamma}_{\text{pool}}$ be the pooled covariance operator, i.e.,

$$\widehat{\Gamma}_{\text{pool}} = \frac{1}{n_1 + n_2} \sum_{k=1}^2 \sum_{i=1}^{n_k} (X_{ki} - \bar{X}_k)^{\otimes 2}.$$

Write $\hat{\gamma}_{\text{pool},j}$ for the j -th eigenvalue of $\widehat{\Gamma}_{\text{pool}}$, and consider the fraction of variance explained at the truncation J as

$$FVE(J) \equiv \frac{\sum_{j=1}^J \hat{\gamma}_{\text{pool},j}}{\sum_{j=1}^{n_1+n_2} \hat{\gamma}_{\text{pool},j}}.$$

Then, for a threshold $\rho \in (0, 1)$, we pick the smallest \hat{J} such that $FVE(\hat{J})$ exceed ρ , that is,

$$\hat{J} \equiv \operatorname{argmin}\{J : FVE(J) \geq \rho\}.$$

This selection strategy is used for the methods QuadInv and QuadMul explained in [Section 5.1](#).

B.5 Implementation of the FoFR estimation

This section describes the truncation level selection for the residual bootstrap used in [Section 5.2](#).

Consider a set J_{res} of candidate truncation levels, e.g., $\mathcal{J}_{\text{res}} = \{1, \dots, 20\}$. We assume $n = Gm$ for simplicity, e.g., $G = 5$, and divide the original sample $\mathcal{D} \equiv \{(Y_i, X_i)\}_{i=1}^n$ into G groups, say $\mathcal{D}_1, \dots, \mathcal{D}_G$. For each $J_{\text{res}} \in \mathcal{J}_{\text{res}}$ and $g = 1, \dots, G$, we perform the following.

1. Use the g -th dataset \mathcal{D}_g as the testing sample and the other datasets $\bigcup_{g' \neq g} \mathcal{D}_{g'}$ as the training samples. The sample sizes are m and $n - m$, and we write $\mathcal{I}_{\text{test}}$ and \mathcal{I}_{tr} for the corresponding index sets.
2. Using the training sample $\{(Y_i, X_i)\}_{i \in \mathcal{I}_{\text{tr}}}$, compute the estimator $\hat{\mathbf{B}}_{\text{tr}, J_{\text{res}}}$ with truncation J_{res} .
3. Using the testing sample $\{(Y_i, X_i)\}_{i \in \mathcal{I}_{\text{test}}}$, compute the prediction error

$$PE_g(J_{\text{res}}) \equiv m^{-1} \sum_{i \in \mathcal{I}_{\text{test}}} \|Y_i - \bar{Y} - \hat{\mathbf{B}}_{\text{tr}, J_{\text{res}}}(X_i - \bar{X})\|^2.$$

We then select an optimal truncation level \hat{K} that minimized the averaged estimated prediction error, i.e.,

$$\hat{J}_{\text{res}} = \operatorname{argmin}_{J_{\text{res}} \in \mathcal{J}_{\text{res}}} G^{-1} \sum_{g=1}^G PE_g(J_{\text{res}}).$$

Upon setting $\hat{J}_{\text{cen}} = \hat{J}_{\text{res}}$, the main truncation level J is chosen by the fraction of variance explained similarly that in [Section B.4](#). We define the fraction of variance explained at the truncation J as

$$FVE(J) \equiv \frac{\sum_{j=1}^J \hat{\gamma}_j}{\sum_{j=1}^n \hat{\gamma}_j}.$$

Then, for a threshold $\rho \in (0, 1)$, we pick the smallest \hat{J} (but no less than \hat{J}_{cen}) such that $FVE(\hat{J})$ exceed ρ , that is,

$$\hat{J} \equiv \operatorname{argmin}\{J \geq \hat{J}_{\text{cen}} : FVE(J) \geq \rho\}.$$